Subglacial water storage and drainage beneath the Fennoscandian and Barents Sea ice sheets

Calvin Shackleton[a*], Henry Patton[a], Alun Hubbard[ab], Monica Winsborrow[a], Jonathan Kingslake[c], Mariana Esteves[a], Karin Andreassen[a], Sarah L. Greenwood[d]
[a] CAGE - Centre for Arctic Gas Hydrate, Environment and Climate, Department of Geosciences, UiT the Arctic University of Norway, 9037 Tromsø, Norway.
[b] Department of Geography and Earth Science, Aberystwyth University, Wales SY23 3DB, UK
[c] Lamont-Doherty Earth Observatory, Columbia University, Palisades, New York 10964, USA
[d] Department of Geological Sciences, Stockholm University, Stockholm, 106 91, Sweden
[*] calvin.s.shackleton@uit.no

Abstract

Subglacial hydrology modulates how ice sheets flow, respond to climate, and deliver meltwater, sediment and nutrients to proglacial and marine environments. Here, we investigate the development of subglacial lakes and drainage networks beneath the Fennoscandian and Barents Sea ice sheets over the Late Weichselian. Utilizing an established coupled climate/ice flow model, we calculate high-resolution, spatio-temporal changes in subglacial hydraulic potential from ice sheet build-up (~37 ka BP) to complete deglaciation (~10 ka BP). Our analysis predicts up to 3,500 potential subglacial lakes, the largest of which was 658 km^2, and over 70% of which had surface areas <10 km^2, comparable with subglacial lake-size distributions beneath the Antarctic Ice Sheet. Asynchronous evolution of the Fennoscandian Ice Sheet into the flatter relief of northeast Europe affected patterns of subglacial drainage, with up to 100 km^3 more water impounded within subglacial lakes during ice build-up compared to retreat. Furthermore, we observe frequent fill/drain cycles within clusters of subglacial lakes at the onset zones and margins of ice streams that would have affected their dynamics. Our results resonate with mapping of large subglacial channel networks indicative of high-discharge meltwater drainage through the Gulf of Bothnia and central Barents Sea. By tracking the migration of meltwater drainage outlets during deglaciation, we constrain locations most susceptible to focussed discharge, including the western continental shelf-break where subglacial sediment delivery led to the development of major trough-mouth fans. Maps of hydraulic potential minima that persist throughout the Late Weichselian reveal potential sites for preserved subglacial lake sediments, thereby defining useful targets for further field-investigation.

Keywords: Subglacial lakes; Basal hydrology; Meltwater drainage; Fennoscandian Ice Sheet; Barents Sea Ice Sheet; Eurasian Ice Sheet Complex; Late Weichselian; Last Glacial Maximum; Glacial geology; Glaciation

Highlights:

- We present modelled subglacial water storage and drainage between 37-10 ka BP
- Up to 3500 potential subglacial lakes predicted during LGM, storing >460 km^3 of water
- Subglacial lake clusters are predicted with potential for fill/drain cycles and flood events
- Persistent lakes over the glaciation define potential sites for preserved sediments
- Catchment evolution and drainage outlet migration reveals subglacial discharge foci

1.0 Introduction

The presence and behaviour of water at the interface between an ice mass and its substrate exerts a fundamental control over many aspects of ice sheet behaviour. Lubrication of the ice-bed interface and subglacial sediment shear strengths are regulated by subglacial water pressure, driving ice flow variability over diurnal and seasonal time-scales (Alley, 1989; Boulton et al., 2001; Weertman, 1972). Refreezing of meltwater at the bed and the resultant release of latent heat also warms and softens basal and englacial ice, leading to enhanced deformation (Arnold and Sharp, 2002; Bell et al., 2014). Subglacial water availability also plays a key role in regulating ice flow, by controlling the distribution of high traction zones (sticky spots) via basal freeze-on (Sergienko and Hulbe, 2011; Trommelen et al., 2014; Winsborrow et al., 2016), and water piracy between neighbouring catchments (Anandakrishnan and Alley, 1997; Carter et al., 2013; Lindbäck et al., 2015). Furthermore, freshwater fluxes exiting sub-marine ice margins directly modulate the rate of mass loss beneath ice shelves and at calving faces through convective-driven melting (Chauché et al., 2014; Jenkins, 2011; Xu et al., 2012). Critically though, changes in ice sheet geometry also strongly influence subglacial hydrological behaviour; even minor changes in ice thickness in areas of low relief can lead to rerouting of basal water flow (Vaughan et al., 2008).

Subglacial lakes are an important component of the subglacial drainage system, and have been studied extensively despite their extreme inaccessibility (Wright and Siegert, 2012). Geophysical and modelling investigations of subglacial lakes and hydrology beneath contemporary ice sheets (Carter et al., 2017; Dowdeswell and Siegert, 2003; Fricker et al., 2007; Hubbard et al., 2004; Lindbäck et al., 2015; Wingham et al., 2006), along with modelling and sedimentary/geomorphic studies of palaeo-subglacial lakes (Christoffersen et al., 2008; Esteves et al., *In Review;* Livingstone et al., 2016; Kuhn et al., 2017), has led to improved understanding of their formation, longevity and influence on ice sheet dynamics. Episodic filling and drainage of subglacial lakes (e.g. Winberry et al., 2009) has been directly linked to accelerations in ice stream velocity (Carter et al., 2013; Stearns et al., 2008) and modifications to background stick-slip cycles in Antarctica (Siegfried et al., 2016). Moreover, internally modulated filling/drainage cycles (Smith et al., 2017; Stearns et al., 2008; Wingham et al., 2006) reveals that subglacial hydrology impacts on ice velocity and mass balance independently of climate forcing. Hence, it is important to consider the mechanisms driving long and short-term behaviour of subglacial lakes and their influence on basal drainage when assessing the current and future stability of ice masses globally.

Palaeo-ice sheets provide an opportunity to investigate the evolution of subglacial hydrological processes over millennial time scales. The Eurasian Ice Sheet Complex (EISC) was the third largest ice mass globally after the Antarctic and the North American ice sheets during the last glaciation, and was comprised of the Celtic Ice Sheet (CIS), the Fennoscandian Ice Sheet (FIS) and the Barents Sea Ice Sheet (BSIS). During the Last Glacial Maximum (LGM), the margins of the EISC reached the continental shelf break along most of the northern and western borders of the Barents Sea, Norway, and the British Isles (Fig. 1). In this study, we focus on the Fennoscandian and Barents Sea sectors of the EISC: independent ice sheet centres which contrasted in their glaciologic, geographic and topographic setting. The majority of the BSIS was grounded below sea level, thereby providing a useful palaeo-analogue for the marine-based West Antarctic Ice Sheet. Conversely, the FIS was largely terrestrial-based, draining ice from the Scandes Mountains to its eastern and southern margins, though with substantial marine terminating-sectors and outlets off the present-day Norwegian and Danish coasts.

Shreve's (1972) subglacial hydraulic potential analysis has been widely applied to infer basal water storage and drainage characteristics beneath both contemporary and palaeo-ice sheets and glaciers, at timescales ranging from days to tens of thousands of years (Alley, 1989; Banwell et al., 2013, 2012; Chu et al., 2016; Lindbäck et al., 2015; Livingstone et al., 2013a; Pattyn, 2008; Sharp et al., 1993; Siegert, 2000; Siegert et al., 2007; Smith et al., 2017; Tulaczyk et al., 2000; Vaughan et al., 2008; Wright et al., 2008; Arnold and Sharp, 2002; Evatt et al., 2006; Gudlaugsson et al., 2017; Livingstone et al., 2013b; Patton et al., 2017a). In this study, we use modelled ice sheet surfaces (Patton et al., 2016, 2017a) and associated isostatic perturbations to reconstruct and investigate the temporal and spatial evolution of potential subglacial drainage routes and subglacial lakes beneath the FIS and BSIS during the build-up to, and retreat from, the LGM. Furthermore, through combined examination of the empirical record, we analyse the potential impacts associated with water routing and storage beneath the ice sheets during deglaciation.

2.0 Methods

2.1 Model output and data

Patton et al. (2016; 2017a) present a first-order thermomechanical model reconstruction of the evolving EISC throughout the Late Weichselian, constrained and validated against a diverse suite of empirical data (Patton et al., 2017a) and independent glacial isostatic adjustment modelling (Auriac et al., 2016). The ice-flow model is fully described in Hubbard (2006a) and consists of a first-order approximation of the Stokes equations, which include longitudinal stress gradients that become increasingly important across steep relief and basal conditions that drive fast-flow (Hubbard, 2000). For the Eurasian domain, the 3D model was applied to a finite-difference grid based on the GEBCO_2014 GRID filtered to a resolution of 10 km, with isostatic loading implemented using an elastic lithosphere/relaxed asthenosphere scheme (Le Meur and Huybrechts, 1996). The first order rheology has been validated against ISMIP-HOM benchmark experiments (Pattyn et al., 2008) and used to successfully reconstruct palaeo-ice sheets across Iceland, Britain and Patagonia (Hubbard et al., 2005; 2006b; 2009; Kuchar et al., 2012; Patton et al., 2013a; 2013b; 2017b). Surface mass balance is determined by a positive degree-day scheme, with both temperature and precipitation adjusting to the evolving ice sheet surface according to prescribed lapse rates derived from multiple regression analyses of modern meteorological observations. Perturbations in climate forcing are scaled against the NGRIP $\partial^{18}O$ ice-core record (Andersen et al., 2004) and sea level forcing applied from a global eustatic reconstruction (Waelbroeck et al., 2002). In this study, we develop the analysis presented by Patton et al. (2017a), and use modelled ice sheet geometry and isostatic adjustments based on output from their model, applied to a resampled (500 m) and filtered GEBCO_2014 Grid (version 20150318, www.gebco.net), to calculate subglacial hydraulic potential over the Late Weichselian glaciation.

2.2 Hydraulic potential calculation

The flow of water at the bed of glaciers and ice sheets is driven by gradients in hydraulic pressure potential (ϕ), which according to Shreve (1972) is a function of the elevation potential and water pressure:

$$\phi = \rho_w g z_b + F \rho_i g (z_s - z_b), \quad (1)$$

where ρ_w is the density of water (1000 kg m^{-3}); g is the acceleration due to gravity (9.81 m s^{-2}); z_b is the bed elevation; ρ_i is the density of ice (917 kg m^{-3}); z_s is the height of the ice sheet surface. The flotation factor (F) is the ratio between subglacial water pressure and the ice overburden pressure, and varies temporally and spatially according to meltwater inputs, drainage system character, basal ice temperature, and the underlying substrate (Andrews et al., 2014; Clarke, 2005).

Boreholes drilled to the bed of the Greenland Ice Sheet reveal a range of subglacial water pressures generally above 90% of the ice overburden pressure. Spatially and temporally averaged (over at least a full melt season) measurements within boreholes of 94.8-96.7% (Doyle et al., 2018); 88-94%; 82-92%; ~100% (Meierbachtol et al., 2013); 85-94% (Thomsen et al., 1991); and 80-110% (Wright et al., 2016) of the overburden are reported, with a mean value of 92.41%. Based on this we adopt an F-value of 0.925, while recognizing that this is a generalisation of the relationship between ice overburden pressure and mean, long-term subglacial water pressure. Banwell et al. (2013) suggest, based on the relationship between modelled run-off and measured proglacial discharge in Greenland, that a value of 0.925 is realistic when averaged over a full melt season. Likewise, Lindbäck et al. (2015) use values ranging from 0.5 to 1.1 to investigate hydrological sensitivities but find a value of 0.925 to be optimal for part of the western sector of the Greenland Ice Sheet.

Equation 1 implicitly demonstrates that ice surface slopes exert ~10-times stronger control on subglacial water flow than basal topography. However, ice sheet surface slopes are generally low and basal slopes can exceed that of the surface by an order of magnitude, and therefore remain a strong influence on the routing and storage of subglacial water, particularly in regions characterised by rugged basal topography. Flow routing tools in the ArcHydro toolbox for ArcGIS 10.5 assume that the steepest gradient in hydraulic potential constrains water flow direction at a given point in eight possible directions. The flow direction of each cell is combined to yield optimal hydrological flowpaths and thereby the predicted drainage network. This method is suitable for the prediction of arborescent channel networks, as the flow routing tools calculate the most efficient path to route water from areas of high to low hydraulic potential. Potential subglacial lake locations are identified by filling local minima in modelled hydraulic potential to their spill point. Subglacial lakes with an area ≤ 2 km^2 are filtered out from the analysis to reduce the impact of interpolation artefacts on results. The capacity for water storage at the bed at each time slice is calculated using the volume to which hydraulic potential requires adjusting to remove the hydraulic potential minima and hence, maximum subglacial lake volume is estimated under the assumption of bank-full conditions. Modelled subglacial drainage maps are generated for discrete time slices at 100-year intervals from 37 to 10 ka BP, and the persistence of hydraulic features is determined by tracking and collating the locations of modelled drainage features through time.

2.3 Methodological and data limitations

Equation 1 couples subglacial water routing to modelled ice sheet thickness and surface gradients in a generalised manner, and furthermore, this approach ignores the reciprocal impact of subglacial water on ice flow. Basal water flow and pressure varies in time and space in response to a multitude of factors including ice sheet characteristics, the nature of the substrate, and meltwater delivery, all of which impact on basal lubrication (Christoffersen et al., 2018; Johnson and Fastook, 2002) and ice flow (Iken, 1981). Also, subglacial water pressure is likely to be much lower close to the ice margin where ice is thinner, and our chosen value for the flotation factor is less representative in this sector where channelized systems may dominate, leading to less reliable predictions of subglacial drainage (Gulley et al., 2012). Meierbachtol et al. (2013) find that conduit pressures of less than 70% of the ice overburden pressure are limited to <10 km from the ice margin, and that subglacial pressures increase to the overburden pressure (i.e. F approaches 1) further into the interior as ice thickness and hydrostatic pressure increases.

Furthermore, coupling feedbacks between the base of the ice sheet and subglacial drainage system are not accounted for, such as lack of basal friction and ice surface flattening over subglacial lakes, and local fluctuations in thermal regime and melt rate. The drainage features modelled in this study are therefore described as potential subglacial routes and lakes and should be considered representative of large-scale patterns of basal drainage. Additionally, conditions that determine subglacial drainage system morphology are absent from this method, including underlying geology, water supply, and sediment load. Limitations for the approach also include the reliability of modelled ice sheet output for calculating hydraulic potential, and interpolation errors in the topography data. An analysis of subglacial lake predictions for an LGM timeslice and the associated GEBCO_2014 source data used for hydraulic potential calculations is presented in Table S1. Furthermore, the digital elevation model (DEM) used for our calculations contains post-glacial sediments and erosion surfaces along with present-day lakes, all of which introduce potential sources of error. Some of these errors can be mitigated by applying a 3 x 3 gaussian filter to the bed DEM and by masking out present-day lakes where appropriate.

2.4 Model sensitivity

A suite of sensitivity experiments was conducted to assess the relative importance of the key parameters influencing the total areal extent of predicted subglacial lakes and the degree to which their spatial extents intersect with the optimum experiment (Table 1). To test the sensitivity of subglacial lakes to changes in water pressure, an experiment using the LGM ice sheet surface (21 ka BP) was conducted, varying the flotation factor (F) using values 0.7, 0.8, 0.925 and 1.0. Model sensitivity to bed roughness was also assessed through varying degrees of bed filtering; the unfiltered GEBCO_2014 DEM, and the results of 1, 2, and 3 passes of a 3 x 3 gaussian filter were used to yield progressive bed smoothing before the hydraulic potential calculation was applied. Sensitivity to modelled basal temperatures was assessed by masking subglacial lake predictions in areas of the bed below -1.5, -0.75, and 0°C (relative to the pressure melting point) and comparing to the optimum experiment without a basal temperature filter. To assess predicted subglacial lake sensitivity to uncertainties in ice model physics, the hydraulic potential analysis was applied under different LGM ice thicknesses, generated using a range of deformation/viscosity (A_0) parameters (Patton et al. 2016). This empirical flow enhancement coefficient is a conventional adaption of Glen's flow law, used to encompass the effects of crystal anisotropy and impurities on bulk ice deformation (Cuffey and Paterson, 2010). The most significant result of modifying strain rates is that softer ice tends to flow faster, resulting in a lower aspect ratio ice sheet and shallower long-profiles of glaciers, while stiffer ice produces thicker glaciers and ice sheets with steeper profiles.

3.0 Results

3.1 Subglacial drainage routing

The modelled subglacial drainage system is organised into linear or dendritic channel networks, which flow in radial patterns from the main ice sheet accumulation centres (Fig. 2a-i). Alongside this radial pattern, topographic features direct large drainage systems along major troughs or around subglacial obstacles. The most extensive subglacial drainage catchments are constrained by their surrounding and underlying topography, and are concentrated beneath palaeo-ice streams such as those occupying the Baltic, Bjørnøyrenna and St. Anna troughs (Figs. 1 and 2). Linear drainage systems close to the ice margins mostly ignore even large-scale topographic features, such as the mountains of Novaya Zemlya, the southern tip of Finland, and present northern coastline of Estonia (Fig. 2d-g) during modelled ice maximum conditions. Extensive and well-connected drainage systems are predicted with increased frequency under ice maximum conditions (Fig. 2c-g), while the dominance of smaller, linear drainage systems is common when ice sheets are smaller and thinner (Fig. 2a,b,h,i).

Some drainage systems are insensitive to fluctuations in ice sheet geometry and remain stable through time. For example, once established, the drainage routes and outlets predicted under the ice streams flowing over the mid-Norwegian shelf (Fig. 1), Hinlopen trough (Fig. 1: HT), and Kvitøya trough east of Svalbard (Fig 1: KvT) remain stable and persist throughout the latter stages of the glaciation (Fig. 2b-g). The present-day Baltic Sea and Gulf of Bothnia host the longest potential drainage network from source to outlet, attaining lengths over 1600 km, and draining the subglacial environment of fast-flowing ice in the Baltic Sea (Fig. 2a-i). This extensive catchment is already active by 30 ka BP and drains subglacial water from terrestrial Sweden and Finland (Fig. 2a). During the modelled build up to LGM conditions, outlet locations remain relatively stable, draining into north-east and coastal Poland at maximum southern ice margin extents (Fig. 2c-f), and shifting northwards to drain into the southern Baltic Sea basin and on into the Gulf of Bothnia as the ice stream retreats (Fig 2g-i).

In the Barents Sea, ice accumulation centres over the islands of Svalbard and Franz Josef Land result in radial drainage during initial ice build-up (Fig. 2a), which is partly funnelled by Storfjordrenna, Bjørnøyrenna, the Franz Victoria Trough, St. Anna Trough, and the surrounding more intricate topographic channels. The modelled ice centres merge and shift southwards towards the central Barents Sea as the ice sheet grows, causing a 90-degree shift in flow direction, shown in the transition between figure 2a-b and figure 2c-d. Bjørnøyrenna hosts the most expansive and hydraulically well-connected drainage system, with a marine-terminating catchment extending from the continental shelf edge into central parts of the Barents Sea (Fig. 2e-g), more than 900 km from source to outlet. As the BSIS retreats through Bjørnøyrenna, drainage routes and outlets migrate eastwards in connection with the shifting ice domes (Fig. 2g,h). The Bjørnøyrenna, Storfjordrenna and north Norwegian Coast Parallel trough catchments experience considerable shifts in marine-terminating drainage outlet locations with changing ice sheet geometry. During ice maximum conditions beginning around 24 ka BP, these three vast catchments drain directly into the Polar North Atlantic, focussed along the western Barents Sea shelf break (Fig. 2c). This ends abruptly following the retreat of the ice margin from the shelf break (after 17 ka BP), after which the outlets are more distributed, draining into the much shallower western Barents Sea (Fig. 2g) and ultimately draining into the central and south-eastern Barents Sea following the break-up of the Fennoscandian-Barents Sea ice saddle (Fig. 2h).

3.2 Potential subglacial lakes

Local hydraulic potential minima, indicative of potential subglacial lakes, are widespread across the beds of the FIS and BSIS. Many subglacial lake locations are regularly predicted in regions of high relief, such as western Novaya Zemlya, Franz Josef Land, Svalbard, the Norwegian coast and across central Scandinavia (Figs. 2a-i; 3a,b). Furthermore, relatively large clusters of subglacial lakes tend to be predicted under thick ice and in inner ice sheet regions, including the central and northern Barents Sea, central Sweden and Finland, the Baltic, and in the Gulf of Bothnia (Fig. 2). In these central areas, predicted subglacial lake locations follow the shifting ice domes, especially in the Barents Sea, where easterly migration is accompanied by an increase in the number and size of region occupied by subglacial lakes in the east of the Barents Sea. As ice thickens between the FIS and BSIS, subglacial lakes are predicted with increased frequency in the southern Barents Sea, especially beneath the thickest ice towards the central sectors (Fig. 2a-g). Subglacial lakes nearer the ice margins are more likely to be found where topography is particularly pronounced, for example, close to the present-day coastlines of northwest Norway and western Novaya Zemlya, and around Svalbard and Franz Josef Land (Fig. 2).

Figure 3 maps subglacial lake persistence, measured as the duration of their presence as a percentage of the total time that each location was ice covered. Many remain stable in the northern Barents Sea (Fig. 3a), Gulf of Bothnia, Baltic Sea and over central Scandinavia and coastal Norway (Fig 3b), with larger and deeper subglacial lakes commonly persisting for over 80% of the time that ice was present. Our results show that subglacial lakes are more persistent in areas of rugged topography such as Franz Josef Land, Svalbard, and the western Norwegian fjords (Fig. 3a,b), and in the stoss sides of major ice-bed topographic obstacles, for example, along the western coast of Novaya Zemlya (Fig. 3a) and the north Estonian coast (Fig. 3b); such topographically-controlled lakes are particularly resilient to changes in ice sheet geometry. Widespread occurrence of potential subglacial lake locations is also predicted in less topographically influenced areas, for example in the relatively flat areas of the northern Barents Sea, surrounding Sentralbankrenna (Fig. 3a), and particularly large examples in the Gulf of Bothnia (Fig. 3b). Some areas lack subglacial lakes, including the relatively shallow areas of Spitsbergenbanken and Murmanskbanken (Fig. 3a), and in the floors of several large troughs including Bjørnøyrenna, the Franz Victoria Trough, Sentraldjupet, and the Norwegian Channel (Fig. 3a,b).

The number of subglacial lakes increases as the ice sheet builds up to its LGM extent (Fig. 4a), with the highest lake count of 3449 (> 2 km^2) occurring at 22.9 ka BP, followed by stepped decreases in lake numbers. A temporary increase in both the number of subglacial lakes (Fig.4a) and volume of water stored within them (Fig. 4b) at the FIS bed occurs immediately before 15 ka BP, following a short re-advance phase and ice surface flattening in the Baltic Sea during overall deglaciation. Fewer lakes are predicted at the bed of the BSIS, peaking later than that of the FIS, with a lingering plateau in lake numbers and water storage through deglaciation (Fig. 4a,b). The relative proportion of the FIS subglacial environment covered by lakes increases from 0.4 % around 10 ka BP to a peak of 1.3 % at 22.9 ka BP. During the lead-up to, and throughout ice-maximum conditions around 24 ka BP, bed coverage by subglacial lakes increases (Fig. 4c) and broadly follows the fluctuating areal extent of the FIS. The BSIS had less of its bed occupied by potential subglacial lakes (Fig. 4c), between 0.1 and 0.4% and with only minor fluctuations over the course of the glaciation. Estimated amounts of water stored within subglacial lakes at the bed of the FIS are much greater during ice build-up than during retreat (Fig. 5), with >100 km^3 difference for the same ice sheet areal extent. Storage of water at the bed of the BSIS (Fig. 5) peaks twice during ice build-up around 34 ka BP and 26 ka BP with approximately linear reductions in water storage capacity throughout retreat.

3.3 Sensitivity analysis

An analysis of the relative importance of key parameters influencing the hydraulic potential modelling (maps presented in Fig. S1) reveals that the greatest sensitivity and difference in subglacial lake coverage is in response to changes in the flotation criterion (Table 1), with an approximately 168,900 km^2 difference in total subglacial lake area between the lowest and highest F-value perturbations. Despite a relatively high range in total subglacial lake area, the spatial correspondence (percentage of subglacial lake area intersecting with the optimum results) between the sensitivity results and optimum experiment remains high, especially for lower F-values. Additionally, the tendency for drainage routes to remain separate, and not merge close to the ice margins (e.g. in Bjørnøyrenna, Fig. 2e) is a symptom of the prescribed high value for the flotation criterion, and therefore increased importance of the ice surface on drainage routing, coupled with steep surface slopes close to the margin.

Subglacial lakes are less sensitive to small-scale perturbations in bed roughness and basal temperatures, with total area differences of 27,500 km^2 and 25,400 km^2 respectively between the highest and lowest sensitivity parameters. Spatial correspondence between subglacial lakes is consistently high between the different bed roughness sensitivity parameters, however, much lower spatial correspondence occurs when results below the pressure melting point are masked out (Table 1). Perturbation in ice flow (deformation/viscosity) parameters yield the smallest spatial extent differences at 12,100 km^2, and strong spatial correspondence with the optimum experiment suggests that the locations of predicted subglacial lakes remains consistent despite ice surface fluctuations. Based on the mostly high spatial correspondence between the optimum experiment and the sensitivity analysis results, we suggest that the locations of predicted subglacial lakes are robust, and that differences in areal coverage are largely driven by fluctuations in the sizes of individual subglacial lakes. Large, deep subglacial lakes are likely to be consistently predicted despite the various perturbations, and will dominate the trends in lake metrics.

4.0 Discussion

Based on the estimation of subglacial hydraulic potential beneath the Fennoscandian and Barents Sea ice sheets, we reconstruct the evolution of subglacial drainage pathways and potential subglacial lake locations through the Late Weichselian. Our reconstructions find potential subglacial lakes to be abundant beneath the former ice sheets, and here the influences on their distribution are discussed and comparison made with empirical evidence for past subglacial hydrology. Finally, we discuss the potential implications that the drainage reconstructions have on ice flow dynamics and beyond the ice margin.

4.1 Influences on subglacial lakes and their distribution

Hydraulic potential gradients are driven by the interplay between bed topography and modelled ice sheet thickness and surface slope. Throughout the glaciation the relationship between, and relative importance of, these drivers change primarily due to fluctuations in ice thickness, ice-divide and margin positions, and surface slopes. Stepped decreases in subglacial lake numbers beneath the FIS during deglaciation (Fig. 4a) are driven by intermittent ice margin retreat/stability, and retreat from areas of high basal roughness (Patton et al., 2017a), which are common across its former bed. The sharp fall in the number of potential subglacial lakes at 18 ka BP, followed by an increase approaching 15 ka BP (Fig. 4a), occurs due to margin retreat in the Baltic and overall thinning, followed by a re-advance phase and ice thickening (Fig. 2). Beneath the BSIS, late ice-dome migration into more topographically rugged eastern sectors of the Barents Sea, and thick ice flowing towards and over the mountains of Novaya Zemlya (Fig. 2) drive the later peak and plateau in subglacial lake numbers (Fig. 4a).

Lake-area frequency distribution for the combined FIS and BSIS throughout their build-up and retreat (Fig. 6a) shows that the majority of predicted subglacial lakes are smaller than 10 km^2 with modal size between 4.3 - 6.8 km^2, similar to those predicted under LGM configurations of the Antarctic Ice Sheet (AIS) (Livingstone et al., 2013a), and those geophysically detected beneath the contemporary AIS (Wright and Siegert, 2012). FIS bed coverage by subglacial lakes is generally above 1 % during the LGM (Fig. 4c), and the peak of 1.3 % at 22.9 ka BP is comparable to 1.2 % of the bed area predicted beneath the present-day Greenland Ice Sheet (Livingstone et al., 2013a). Higher numbers and a greater portion of the bed covered by lakes beneath the FIS again are likely driven by a higher subglacial bed roughness when compared to the BSIS, which had large portions underlain by relatively smooth bed (Fig.1). Moreover, the flat surface of present-day lakes in the DEM precludes the prediction of subglacial lakes in these basins, and so in reality the percentage of the ice bed occupied by subglacial lakes for the FIS is likely to have been considerably greater given the abundance of present-day lakes (covering >100,000 km^2; www.ngdc.noaa.gov) across Fennoscandia (Fig. 3b).

The differences in potential subglacial lake coverage between the FIS and BSIS could also be explained by the post-glacial draping of marine sediments and sparse coverage and accuracy of bathymetric data in the Barents Sea, compared to the resolution, accuracy, and density of terrestrial data that cover the former FIS bed. However, the large, smooth troughs characteristic of the Barents Sea were inherited from earlier glaciations and underwent intense erosion during the lead-up to the LGM, and therefore were glacially smoothed prior to the inferred period of meltwater activity. Present sedimentation rates in the Barents Sea are generally low at c. 2-5 cm ka^{-1}, increasing to 15-20 cm ka^{-1} in near coastal areas (Elverhøi et al., 1989). Predicted subglacial lake numbers could potentially be higher with the provision of more accurate bathymetric and terrestrial data, although the total water storage capacity of subglacial lakes at the bed is unlikely to be significantly affected by DEM resolution or Holocene sediment draping.

For comparable ice sheet dimensions the volume of water stored within subglacial lakes at the bed of the FIS is up to twice as much (>100 km^3 greater) during ice build-up than during retreat (Fig. 5). This occurs despite a uniform relationship between ice-sheet area and the area of the bed occupied by lakes

(Fig. 6b). However, subglacial lakes inherited from previous ice sheet configurations could persist through changes in ice-sheet geometry due to the postive feedback effect of ice-surface flattening above subglacial lakes reinforcing their stability (Livingstone et al. 2013a). This effect is not captured in our approach due to the absence of dynamic ice-hydrological coupling within the ice-sheet model, and so the disparity between water volumes stored within subglacial lakes beneath the advancing and retreating FIS is likely to have been lower. Nevertheless, the migration of FIS ice domes into the flatter sectors of eastern Fennoscandia led to lower volumes of water storage during deglaciation. It is also likely that subglacial lakes were deeper and more abundant during ice build-up, as the steeper surface slopes of a retreating ice sheet promote shallower, less stable subglacial lakes, with the potential for impacting on the rate of ice retreat through hydraulically driven modulation of ice velocties.

4.2 Affinity with the empirical record

The geomorphological record of subglacial hydrology is influenced by the geology of the former ice-bed, and is likely to be biased towards the most erosive and persistent hydraulic activity. The preservation potential for evidence of subglacial lakes is low, especially for small, fast-circulation lakes which exist only on short time scales and account for a large proportion of the predicted subglacial lakes in this study (Fig. 3a,b). However, recent work identifying the geomorphological and sedimentological records of subglacial lakes and downstream landforms such as meltwater channels and eskers has successfully reconstructed former hydraulic conditions (Kuhn et al., 2017; Livingstone et al., 2015, 2012; Livingstone and Clark, 2016; Simkins et al., 2017), in particular those related to rapid, high-discharge drainage events. In the Barents Sea and Fennoscandia recent empirial studies (Bjarnadóttir et al., 2016; Esteves et al., 2017, *In Review;* Greenwood et al., 2016; 2017) enable the assessment of our predicted routing and lake locations against the palaeo-record of subglacial meltwater activity.

Our analysis reveals that the Gulf of Bothnia was a focal point for the routing and storage of subglacial meltwater over much of the last glaciation; a result that resonates strongly with the empirical record. Large, persistent subglacial lakes are predicted in the north-western and southern Gulf of Bothnia (Fig. 3b), along with water routing through the area throughout ice occupancy (Fig. 2a-i). Between the predicted subglacial lakes (Fig. 7a), a suite of subglacial meltwater landforms are observed, including eskers and meltwater channels up to 4 km wide (Clason et al., 2016; Greenwood et al., 2017, 2016). High energy and high discharge meltwater systems are invoked to explain the observed channel features (Greenwood et al., 2016), and a large, periodically draining subglacial lake proposed upstream of the drainage features (Greenwood et al., 2017) is supported by our results (Fig. 7a). A source of periodic or steady water injections to the clearly dynamic subglacial hydraulic system through this area is provided by the high number of subglacial lakes predicted here (Fig. 7a). Further, sudden large inputs of water to the drainage systems might lead to hydraulic overcapacity, initiating the formation of R-channels which infill with sediments to leave behind eskers following the decreases in discharge associated with complete drainage of a subglacial lake or termination of a flood event. The large number of eskers across Fennoscandia (Stroeven et al., 2016) may be related to the propensity of the landscape for subglacial lake formation as a source of time-varying meltwater fluxes. Compatibly, eskers are associated to the areas downstream of subglacial lakes beneath the North American palaeo-ice sheet (Livingstone et al., 2016).

Geomorphological and sedimentological investigations in the central Barents Sea also reveal several clusters of interconnected palaeo-subglacial lakes, meltwater channels, and eskers (Bjarnadóttir et al., 2017; Esteves et al., 2017, *In Review*). We predict subglacial lakes in several sites of mapped basins that are upstream of, and interlinking, large meltwater channels that feed into the Sentralbankrenna Ice Stream bed (Fig. 7b). It is suggested that the subglacial hydrology of this region was characterised by fill/drain cycles and periodic outburst flooding from hypothesised subglacial lakes (Bjarnadóttir et al., 2016; Esteves et al., 2017; *In Review*), compatible with the clusters of lakes predicted in this study. The lower number of times subglacial lakes are predicted at sites in the central Barents Sea compared to those in the Gulf of Bothnia (Fig. 7) tentatively suggests that their stability was susceptible to fluctuations in the configuration of overlying ice. Wider analysis of the association between meltwater geomorphology and predicted lakes gives confidence to reconstructions of subglacial hydrology and its impacts on ice flow. Inversely, sites of persistent subglacial lakes (Figs. 3a,b; 7a,b) are also more likely to contain geomorphological evidence of hydraulic activity and might make good candidates for geophysical/sedimentological surveys in search of palaeo-subglacial lakes.

4.3 Impacts of subglacial hydrology on ice dynamics

Subglacial lakes have been detected at the onset of ice streams in Antarctica (Bell et al., 2007; Fricker et al., 2007), and directly influence ice flow velocities through drainage events (Stearns et al., 2008) which can occur periodically due to natural instability (Evatt et al., 2006; Pattyn, 2008; Wingham et al., 2006). Hydraulically connected clusters of subglacial lakes modify basal stick-slip behaviour, and are associated with hydrologically-induced sticky-spots and effective pressure modulation through regulation of meltwater supply to the bed (Siegfried et al., 2016; Smith et al., 2017). A large number of both persistent and short-lived subglacial lakes are predicted at the onset of and draining into the beds of Fennoscandian and Barents Sea ice streams, including those occupying the Franz Victoria Trough, Sentralbankrenna, Djuprenna (Fig. 3a), Vestfjorden/Traenadjupet, and the Baltic (Fig. 3b). Although our approach lacks coupling between subglacial meltwater and ice dynamics, the abundance of predicted subglacial lakes connected to these modelled ice streams show the potential for impacts on ice dynamics by regulating meltwater supply to the bed, and clusters of predicted lake locations indicate the potential for interconnected subglacial lake systems analogous to those observed beneath contemporary ice sheets (e.g. Smith et al., 2017; Wingham et al., 2006) and at deglaciated beds (Nitsche et al., 2013; Simkins et al., 2017). Furthermore, a reduced capacity for water storage at the bed of retreating ice sheets, as demonstrated here for the FIS during deglaciation (Fig. 5), could limit the effect of periodic modifications to ice-flow through subglacial lake filling and draining. This would promote a more moderate response to increasing/decreasing meltwater inputs and associated impacts on ice flow.

Previous studies demonstrate that FIS flow, and consequently ice thickness, is highly sensitive to basal meltwater (Arnold and Sharp, 2002; Clason et al., 2014; Gudlaugsson et al., 2017), and predictions of large, highly persistent lakes in the rugged topography of Fennoscandia and eastern

Novaya Zemlya (Gudlaugsson et al., 2017) are in general agreement with our predictions. Our results demonstrate a greater frequency of less-persistent subglacial lakes especially in the Barents Sea and eastern Fennoscandia (Fig. 3a,b) which are prone to drainage with small shifts in ice geometry. Clason et al. (2016) suggest that ice flow and grounding line retreat through the Bothnian Sea was influenced by surface meltwater enhanced basal sliding, which is supported by evidence for high-discharge subglacial meltwater conduits (Greenwood et al., 2017, 2016). A propensity for subglacial lake formation in the Gulf of Bothnia and surrounding areas (Fig. 4b) suggests that surface meltwater penetrating to the bed could have been stored in subglacial lakes and released on varying timescales, further modulating the stability and dynamic activity of the ice stream. Similarly, given the evidence for high-discharge subglacial meltwater systems in the central Barents Sea (Bjarnadóttir et al., 2017; Esteves et al., 2017), it it likely that ice flow of the Sentralbankrenna Ice Stream, and the neighbouring Bjørnøyrenna Ice Stream (Fig. 1), would have been regulated by the filling and draining of the subglacial lakes predicted in their onset zones (Fig. 7b). Evidence for highly dynamic ice stream activity is recorded in the geomorphology of their former beds, with cross-cutting sets of mega-scale glacial lineations indicating numerous switches in flow direction during the LGM (Piasecka et al., 2016). Furthermore, grounding zone wedges containing evidence for ice-marginal subglacial meltwater dicharge suggest cycles of ice margin retreat, stability, and re-advance influenced by sustained basal hydrological activity during overall retreat (Bjarnadóttir et al., 2014; Esteves et al., 2017; Newton and Huuse, 2017).

The routing of water also has implications for the dynamics of overlying ice, as shallow surface slopes render subglacial water routing extremely sensitive to minor shifts in ice sheet geometry. These areas are susceptible to rerouting of drainage towards or away from individual catchments, with the potential for hydraulic regulation of fast ice flow, as has been observed in present-day Antarctica and Greenland (Anandakrishnan and Alley, 1997; Carter et al., 2013; Lindbäck et al., 2015; Vaughan et al., 2008). Empirical based reconstructions of ice stream dynamics in Bjørnøyrenna suggest frequent major switches in ice flow directions during the LGM (Piasecka et al., 2016) and surging behaviour during retreat (Andreassen et al., 2014; Bjarnadóttir et al., 2014) which, in combination with shifting ice divides, may have been driven by fluctuating meltwater routing and lake fill/drain cycles given the high number of subglacial lake clusters predicted at the onset of, and in the tributaries to the former ice stream. This is supported by evidence for vast subglacial meltwater networks and interlinked subglacial lakes surrounding the Sentralbankrenna tributary ice stream (Bjarnadóttir et al., 2016; Esteves et al., 2017, *In Review*). Geomorphic evidence is generally in agreement with our modelling results which predict highly dynamic drainage systems with the potential for upstream subglacial lakes feeding into drainage systems with significant temporal and spatial variations in water routing.

4.4 Potential impacts beyond the ice margin

The locations of subglacial drainage outlets are transient and migrate in response to changes in ice margin position, ice sheet configuration and geometry, and shifts in proximity to/contact with the oceans which, in turn, are influenced by eustatic sea-level changes and ice stream discharge. Figure 8 maps subglacial drainage outlets, colour coded by catchment size, between maximum ice extent at 22.7 ka BP and through to full deglaciation at 10 ka BP. Given the large catchment size of some predicted subglacial drainage systems (a maximum of 327,000 km^2 beneath the Baltic Sea Ice Stream and 224,000 km^2 beneath the Bjørnøyrenna Ice Stream) it is likely that they were responsible for concentrated sediment deposition and focussed inputs of cold, fresh water to the oceans and Eurasian continent, especially during deglaciation.

Sudden drops in subglacial water storage capacity, for example at 23 ka BP and 15 ka BP (Fig. 4b), result in over 100 km^3 of freshwater input to the subglacial system fed from subglacial lakes alone, which is subsequently routed towards the margins. Outlet positions and subglacial catchment sizes are therefore important when considering the influence of retreating ice sheets on proglacial landscape evolution and where glacially eroded sediments are transported and deposited. Additionally, the estimated combined volume of water stored within subglacial lakes at the beds of the FIS and BSIS ranges from 36 to 462 km^3 (Fig. 4b), highlighting the important function of subglacial lakes as both a perennial store and source of freshwater, dependent on ice-sheet geometry. In comparison, estimated total volumes of water stored beneath the FIS and BSIS (Fig. 5) are less than the ~1000 km^3 predicted beneath LGM configurations of the North American Ice Sheet (Livingstone et al., 2013b) and considerably less than the 9000 – 16,000 km^3 estimated beneath the contemporary AIS (Wright and Siegert, 2012).

Nearly half of the total LGM ice sheet configuration terminated in marine outlets (Fig. 8), which subsequently increased through deglaciation. The strongest concentrations of meltwater and sediment delivery to marine-terminating sectors occurred at the continental shelf break west of Bjørnøyrenna, towards the Bjørnøyrenna Trough Mouth Fan (TMF; Fig. 8), the largest glacial sediment depocentre in the Arctic (Vorren et al., 2011). Outlets draining catchments approaching 300,000 km^2 are predicted consistently here throughout ice margin retreat (Fig. 8), and these would have been the primary source of sediments to the upper slope, and potentially to enhanced deposition conducive to slope failures (e.g. Lucchi et al., 2012, 2013), thereby influencing slope stability. Furthermore, discharge of meltwater with a high concentration of suspended sediments may flow hyperpycnally along the seabed and initiate turbidity currents (Piper and Normark, 2009), thereby directly contributing to both the quantity and architecture of proglacial marine sediments accumulated within TMFs.

The TMF associated with the neighbouring Storfjordrenna Ice Stream contains well-documented sedimentological evidence for intensive meltwater plume activity (Llopart et al., 2015). Distinct meltwater signals between three hypothesised sub-ice stream lobes here (Pedrosa et al., 2011) is supported by the outlet positions and distinct migration paths predicted in this study (Fig. 8). Stable drainage outlets of substantial size might also have contributed to three partly merged sediment depocenters off the mid-Norwegian Shelf (Fig. 8), although material from the most southern depocentre (and largest catchment area outlets) has been removed by mass slides in Storegga (Dahlgren et al., 2005). Where major catchments outlet onto terrestrial regions, they contributed to the formation of large proglacial lakes and river networks (Patton et al., 2017a). Large catchment outlets in the Baltic leading up to the Younger Dryas (11.7 ka BP) are also accordant with the initiation of and precursors to the Baltic Ice Lake around 14.2 ka BP (Mangerud et al., 2004).

5.0 Conclusions

Through the application of well-constrained ice sheet modelling output, we demonstrate the abundance of potential sites for subglacial lake formation and drainage pathways beneath the Fennoscandian and Barents Sea ice sheets through the Last Glacial Maximum (37-10 ka BP). During peak glaciation c. 22.7 ka BP up to 3500 subglacial lake locations are predicted, accounting for 38,580 km^2 of the subglacial domain. Throughout deglaciation, predicted subglacial lake locations resonate with recent geomorphological mapping, evidencing pronounced water fluxes beneath both ice sheets, and indicating that subglacial meltwater played a major role in governing dynamic and rapid ice-sheet retreat. Several cluster-sites of potential subglacial lakes are predicted at the onset of, and in the banks surrounding, the Bjørnøyrenna, Franz-Victoria Trough, Baltic Sea, and Norwegian Coast Parallel palaeo-ice streams, suggesting these ice-sheet catchments were susceptible to hydraulic regulation. Lower volumes of water impounded beneath the FIS during ice retreat demonstrates the potential for shallower, unstable subglacial lakes under its retreating ice geometry, with implications for the supply of meltwater to the bed and impacts on ice flow surrounding, and downstream of, major Fennoscandian subglacial lakes.

Transient model outputs reveal the migration paths of subglacial catchment outlets, from which concentrations of sediments and freshwater exited the ice sheet system. While the ice margin lay adjacent to the continental shelf edge, these shifting outlets would have contributed to the build-up and architecture of sediments within the adjacent trough mouth fans, the most significant of which lay beneath the Bjørnøyrenna ice stream with a catchment reach of >900 km. Subglacial lake persistency maps integrated over the full Late Weichselian glaciation reveal multiple sites for long-lived, and potentially preserved, subglacial lakes. These locations represent key targets for further geophysical/sedimentological investigations.

6.0 Acknowledgements

This research is part of the Centre for Arctic Gas Hydrate, Environment and Climate and was supported by the Research Council of Norway through its Centres of Excellence funding scheme grant No. 223259. The ice sheet modelling outputs used were also supported by the PetroMaks project "Glaciations in the Barents Sea area (GlaciBar)" (grant No. 200672). We thank two anonymous reviewers for their constructive feedback on the manuscript.

7.0 References

Alley, R.B., 1989. Water-pressure coupling of sliding and bed deformation: 1. Water system. J. Glaciol. 35, 108–118.

Anandakrishnan, S., Alley, R.B., 1997. Stagnation of Ice Stream C, West Antarctica by water piracy. Geophys. Res. Lett. 24, 265. doi:10.1029/96GL04016

Andersen, K.K., Azuma, N., Barnola, J.M., Bigler, M., Biscaye, P., Caillon, N., Chappellaz, J., Clausen, H.B., Dahl-Jensen, D., Fischer, H., Flückiger, J., Fritzsche, D., Fujii, Y., Goto-Azuma, K., Grønvold, K., Gundestrup, N.S., Hansson, M., Huber, C., Hvidberg, C.S., Johnsen, S.J., Jonsell, U., Jouzel, J., Kipfstuhl, S., Landais, A., Leuenberger, M., Lorrain, R., Masson-Delmotte, V., Miller, H., Motoyama, H., Narita, H., Popp, T., Rasmussen, S.O., Raynaud, D., Rothlisberger, R., Ruth, U., Samyn, D., Schwander, J., Shoji, H., Siggard-Andersen, M.L., Steffensen, J.P., Stocker, T., Sveinbjörnsdóttir, A.E., Svensson, A., Takata, M., Tison, J.L., Thorsteinsson, T., Watanabe, O., Wilhelms, F., White, J.W.C., 2004. High-resolution record of Northern Hemisphere climate extending into the last interglacial period. Nature 431, 147–151. doi:10.1038/nature02805

Andreassen, K., Winsborrow, M.C.M., Bjarnadóttir, L.R., Rüther, D.C., 2014. Ice stream retreat dynamics inferred from an assemblage of landforms in the northern Barents Sea. Quat. Sci. Rev. 92, 246–257. doi:10.1016/j.quascirev.2013.09.015

Andrews, L.C., Catania, G.A., Hoffman, M.J., Gulley, J.D., Lüthi, M.P., Ryser, C., Hawley, R.L., Neumann, T.A., 2014. Direct observations of evolving subglacial drainage beneath the Greenland Ice Sheet. Nature 514, 80–83. doi:10.1038/nature13796

Arnold, N., Sharp, M., 2002. Flow variability in the Scandinavian ice sheet: Modelling the coupling between ice sheet flow and hydrology. Quat. Sci. Rev. 21, 485–502. doi:10.1016/S0277-3791(01)00059-2

Auriac, A., Whitehouse, P.L., Bentley, M.J., Patton, H., Lloyd, J.M., Hubbard, A., 2016. Glacial isostatic adjustment associated with the Barents Sea ice sheet: A modelling inter-comparison. Quat. Sci. Rev. 147, 122–135. doi:10.1016/j.quascirev.2016.02.011

Banwell, A.F., Arnold, N.S., Willis, I.C., Tedesco, M., Ahlstrøm, A.P., 2012. Modeling supraglacial water routing and lake filling on the Greenland Ice Sheet. J. Geophys. Res. Earth Surf. 117, F04012. doi:10.1029/2012JF002393

Banwell, A.F., Willis, I.C., Arnold, N.S., 2013. Modeling subglacial water routing at Paakitsoq, W Greenland. J. Geophys. Res. Earth Surf. 118, 1282–1295. doi:10.1002/jgrf.20093

Bell, R.E., Paden, J., Tinto, K., Das, I., Wolovick, M., Chu, W., Creyts, T.T., Frearson, N., Abdi, A., Paden, J.D., 2014. Deformation, warming and softening of Greenland's ice by refreezing meltwater. Nat. Geosci. 7, 497–502. doi:10.1038/ngeo2179

Bell, R.E., Studinger, M., Shuman, C.A., Fahnestock, M.A., Joughin, I., 2007. Large subglacial lakes in East Antarctica at the onset of fast-flowing ice streams. Nature 455, 904-907. doi:10.1038/nature05554

Bjarnadóttir, L.R., Winsborrow, M.C.M., Andreassen, K., 2017. Large subglacial meltwater features in the central Barents Sea. Geology 45, 1–45. doi:10.1111/bor.12142

Bjarnadóttir, L.R., Winsborrow, M.C.M., Andreassen, K., 2014. Deglaciation of the central Barents Sea. Quat. Sci. Rev. 92, 208–226. doi:10.1016/j.quascirev.2013.09.012

Boulton, G.S., Dobbie, K.., Zatsepin, S., 2001. Sediment deformation beneath glaciers and its coupling to the subglacial hydraulic system. Quat. Int. 86, 3–28. doi:10.1016/S1040-6182(01)00048-9

Carter, S.P., Fricker, H.A., Siegfried, M.R., 2017. Antarctic subglacial lakes drain through sediment-floored canals: Theory and model testing on real and idealized domains. Cryosph. 11, 381–405. doi:10.5194/tc-2016-74

Carter, S.P., Fricker, H.A., Siegfried, M.R., 2013. Evidence of rapid subglacial water piracy under Whillans Ice Stream, West Antarctica. J. Glaciol. 59, 1147–1162. doi:10.3189/2013JoG13J085

Chauché, N., Hubbard, A., Gascard, J.-C., Box, J.E., Bates, R., Koppes, M., Sole, A., Christoffersen, P., Patton, H., 2014. Ice–ocean interaction and calving front morphology at two west Greenland tidewater outlet glaciers. Cryosph. 8, 1457–1468. doi:10.5194/tc-8-1457-2014

Christoffersen, P., Tulaczyk, S., Wattrus, N.J., Peterson, J., Quintana-Krupinski, N., Clark, C.D., Sjunneskog, C., 2008. Large subglacial lake beneath the Laurentide Ice Sheet inferred from sedimentary sequences. Geology 36, 563–566. doi:10.1130/G24628A.1

Christoffersen, P., Pettersson, R., Hubbard, A., Doyle, S.H., Grigsby, S., 2018. Cascading lake drainage on the Greenland Ice Sheet triggered by tensile shock and fracture. Nat. Commun. 9, 1064. doi:10.1038/s41467-018-03420-8

Chu, W., Creyts, T.T., Bell, R.E., 2016. Rerouting of subglacial water flow between neighboring glaciers in West Greenland. J. Geophys. Res. 121, 925–938. doi:10.1002/2015JF003705

Clarke, G.K.C., 2005. Subglacial Processes. Annu. Rev. Earth Planet. Sci. 33, 247–276. doi:10.1146/annurev.earth.33.092203.122621

Clason, C.C., Applegate, P.J., Holmlund, P., 2014. Modelling Late Weichselian evolution of the Eurasian ice sheets forced by surface meltwater-enhanced basal sliding. J. Glaciol. 60, 29–40. doi:10.3189/2014JoG13J037

Clason, C.C., Greenwood, S.L., Selmes, N., Lea, J.M., Jamieson, S.S.R., Nick, F.M., Holmlund, P., 2016. Controls on the early Holocene collapse of the Bothnian Sea Ice Stream. J. Geophys. Res. Earth Surf. 121, 2494–2513. doi:10.1002/2016JF004050

Cuffey, K.M., Paterson, W.S.B., 2010. The Physics of Glaciers, fourth ed. Butterworth-Heinemann, Oxford.

Dahlgren, K.I.T., Vorren, T.O., Stoker, M.S., Nielsen, T., Nygård, A., Sejrup, H.P., 2005. Late Cenozoic prograding wedges on the NW European continental margin: Their formation and relationship to tectonics and climate. Mar. Pet. Geol. 22, 1089–1110. doi:10.1016/j.marpetgeo.2004.12.008

Dowdeswell, J.A., Siegert, M.J., 2003. The physiography of modern Antarctic subglacial lakes. Glob. Planet. Change 35, 221–236. doi:10.1016/S0921-8181(02)00128-5

Doyle, S.H., Hubbard, B., Christoffersen, P., Young T. J., Hofstede, C., Bougamont M., Box J. E., Hubbard A., 2018. Physical Conditions of Fast Glacier Flow: 1 . Measurements From Boreholes Drilled to the Bed of Store Glacier, West Greenland. J. Geophys. Res. Earth Surf. 123.

Elverhøi, A., Pfirman, S.L., Solheim, A., Larssen, B.B., 1989. Glaciomarine sedimentation in epicontinental seas exemplified by the northern Barents Sea. Mar. Geol. 85, 225–250. doi:10.1016/0025-3227(89)90155-2

Esteves, M., Bjarnadóttir, L.R., Winsborrow, M.C.M., Shackleton, C.S., Andreassen, K., 2017. Retreat patterns and dynamics of the Sentralbankrenna glacial system , Central Barents Sea. Quat. Sci. Rev. 169, 131–147. doi:10.1016/j.quascirev.2017.06.004

Esteves, M., Rüther, D., Winsborrow, M.C.M., Livingstone, S.J., Shackleton, C.S., Andreassen, K., Hong, W.-L. and Knies, J. *In Review.* An interconnected palaeo-subglacial lake system in the central Barents Sea.

Evatt, G., Fowler, A., Clark, C., Hulton, N.R., 2006. Subglacial floods beneath ice sheets. Philos. Trans. R. Soc. London A Math. Phys. Eng. Sci. 364.

Evatt, G.W., Fowler, A.C., Clark, C.D., Hulton, N.R.J., 2006. Subglacial floods beneath ice sheets. Philos. Trans. A. Math. Phys. Eng. Sci. 364, 1769–94. doi:10.1098/rsta.2006.1798

Fricker, H.A., Scambos, T., Bindschadler, R., Padman, L., 2007. An active subglacial water system in West Antarctica mapped from space. Science 315, 1544–1548. doi:10.1126/science.1136897

Greenwood, S.L., Clason, C.C., Jakobsson, M., 2016. Ice-flow and meltwater landform assemblages in the Gulf of Bothnia. Geol. Soc. London Mem. 46, 321–324. doi:10.1144/M46.163

Greenwood, S.L., Clason, C.C., Nyberg, J., Jakobsson, M., Holmlund, P., 2017. The Bothnian Sea ice stream: early Holocene retreat dynamics of the south-central Fennoscandian Ice Sheet. Boreas 46, 346–362. doi:10.1111/bor.12217

Gudlaugsson, E., Humbert, A., Andreassen, K., Clason, C.C., Kleiner, T., Beyer, S., 2017. Eurasian ice-sheet dynamics and sensitivity to subglacial hydrology. J. Glaciol. 63, 556–564. doi:10.1017/jog.2017.21

Gulley, J.D., Grabiec, M., Martin, J.B., Jania, J., Catania, G., Glowacki, P., 2012. The effect of discrete recharge by moulins and heterogeneity in flow-path efficiency at glacier beds on subglacial hydrology. J. Glaciol. 58, 926–940. doi:10.3189/2012JoG11J189

Hubbard, A., 2000. The verification and significance of three approaches to longitudinal stresses in high-resolution models of glacier flow. Geogr. Ann. Ser. A Phys. Geogr. 82, 471–487. doi:10.1111/j.0435-3676.2000.00135.x

Hubbard, A., Lawson, W., Anderson, B., Hubbard, B. & Blatter, H. 2004. Evidence for subglacial ponding across Taylor Glacier, Dry Valleys, Antarctica. Annals of Glaciology 39, 79-84.

Hubbard, A., Hein, A.S., Kaplan, M.R., Hultun, N.R.J., Glasser, N., 2005. A modelling reconstruction of the last glacial maximum ice sheet and its deglaciation in. Geogr. Ann. 87, 375–391.

Hubbard, A. 2006a. The validation and sensitivity of a model of the Icelandic ice sheet. Quaternary Science Reviews 25 (17-18), 2297-2313.

Hubbard, A., Sugden, D., Dugmore, A., Norddahl, H., Pétursson, H.G., 2006b. A modelling insight into the Icelandic Last Glacial Maximum ice sheet. Quat. Sci. Rev. 25, 2283–2296. doi:10.1016/j.quascirev.2006.04.001

Hubbard, A., Bradwell, T., Golledge, N., Hall, A., Patton, H., Sugden, D., Cooper, R., Stoker, M., 2009. Dynamic cycles, ice streams and their impact on the extent, chronology and deglaciation of the British–Irish ice sheet. Quat. Sci. Rev. 28, 758–776. doi:10.1016/j.quascirev.2008.12.026

Iken, A., 1981. The effect of the subglacial water pressure on the sliding velocity of a glacier in an idealized numerical model. J. Glaciol. 27, 407–421. doi:10.3198/1981JoG27-97-407-421

Jenkins, A., 2011. Convection-Driven Melting near the Grounding Lines of Ice Shelves and Tidewater Glaciers. J. Phys. Oceanogr. 41, 2279–2294. doi:10.1175/JPO-D-11-03.1

Johnson, J., Fastook, J.L., 2002. Northern Hemisphere glaciation and its sensitivity to basal melt water. Quat. Int. 95, 65–74. doi:10.1016/S1040-6182(02)00028-9

Kuhn, G., Hillenbrand, C.-D., Kasten, S., Smith, J.A., Nitsche, F.O., Frederichs, T., Wiers, S., Ehrmann, W., Klages, J.P., Mogollon, J.M., 2017. Evidence for a palaeo-subglacial lake on the Antarctic continental shelf. Nat. Commun. 8, 15591. doi:10.1038/ncomms15591

Kuchar, J., Milne, G., Hubbard, A., Patton, H., Bradley, S., Shennan, I., Edwards, R., 2012. Evaluation of a numerical model of the British – Irish ice sheet using relative sea-level data: implications for the interpretation of trimline observations. J. Quat. Sci. 27, 597–605. doi:10.1002/jqs.2552

Le Brocq, A.M., Payne, A.J., Siegert, M.J., Alley, R.B., 2009. A subglacial water-flow model for West Antarctica. J. Glaciol. 55, 879–888. doi:10.1063/1.2756072

Le Meur, E., Huybrechts, P., 1996. A comparison of different ways of dealing with isostasy: examples from modelling the Antarctic ice sheet during the last glacial cycle. Ann. Glaciol. 23, 309–317. doi:10013/epic.12717.d001

Lindbäck, K., Pettersson, R., Hubbard, A.L., Doyle, S.H., van As, D., Mikkelsen, A.B., Fitzpatrick, A.A., 2015. Subglacial water drainage, storage, and piracy beneath the Greenland Ice Sheet. Geophys. Res. Lett. 42, 7606–7614. doi:10.1002/2015GL065393

Livingstone, S.J., Clark, C.D., 2016. Morphological properties of tunnel valleys of the southern sector of the Laurentide Ice Sheet and implications for their formation. Earth Surf. Dyn. 4, 567–589. doi:10.5194/esurf-4-567-2016

Livingstone, S.J., Clark, C.D., Piotrowski, J.A., Tranter, M., Bentley, M.J., Hodson, A., Swift, D.A., Woodward, J., 2012. Theoretical framework and diagnostic criteria for the identification of palaeo-subglacial lakes. Quat. Sci. Rev. 53, 88–110. doi:10.1016/j.quascirev.2012.08.010

Livingstone, S.J., Clark, C.D., Tarasov, L., 2013. Modelling North American palaeo-subglacial lakes and their meltwater drainage pathways. Earth Planet. Sci. Lett. 375, 13–33. doi:10.1016/j.epsl.2013.04.017

Livingstone, S.J., Clark, C.D., Woodward, J., Kingslake, J., 2013. Potential subglacial lake locations and meltwater drainage pathways beneath the Antarctic and Greenland ice sheets. Cryosphere 7, 1721–1740. doi:10.5194/tc-7-1721-2013

Livingstone, S.J., Storrar, R.D., Hillier, J.K., Stokes, C.R., Clark, C.D., Tarasov, L., 2015. An ice-sheet scale comparison of eskers with modelled subglacial drainage routes. Geomorphology 246, 104–112. doi:10.1016/j.geomorph.2015.06.016

Livingstone, S.J., Utting, D.J., Ruffell, A., Clark, C.D., Pawley, S., Atkinson, N., Fowler, A.C., 2016. Discovery of relict subglacial lakes and their geometry and mechanism of drainage. Nat. Commun. 7. doi:10.1038/ncomms11767

Llopart, J., Urgeles, R., Camerlenghi, A., Lucchi, R.G., Rebesco, M., De Mol, B., 2015. Late Quaternary development of the Storfjorden and Kveithola Trough Mouth Fans, northwestern Barents Sea. Quat. Sci. Rev. 129, 68–84. doi:10.1016/j.quascirev.2015.10.002

Lucchi, R.G., Camerlenghi, A., Rebesco, M., Colmenero-hidalgo, E., Sierro, F.J., Sagnotti, L., Urgeles, R., Melis, R., Morigi, C., Barcena, M.A., Giorgetti, G., Villa, G., Persico, D., Flores, J.A., Rigual-Hernandez, A.S., Pedrosa, M.T., Macri, P., Caburlotto, A., 2013. Postglacial sedimentary processes on the Storfjorden and Kveithola trough mouth fans : Significance of extreme glacimarine sedimentation. Glob. Planet. Change 111, 309–326.

Lucchi, R.G., Pedrosa, M.T., Camerlenghi, A., Urgeles, R., De Mol, B., Rebesco, M., 2012. Recent Submarine Landslides on the Continental Slope of Storfjorden and Kveithola Trough-Mouth Fans (North West Barents Sea), In: Yamada, Y., Kawamura, K., Ikehara, K., Ogawa, Y., Urgeles, R.,Mosher, D., Chaytor, J., Strasser, M. (Eds.), Submarine Mass Movements and Their Consequences. Advances in Natural and Technological Hazards Research, Springer Science Book Series, 31, 735-745. doi:10.1007/978-94-007-2162-3

Mangerud, J., Jakobsson, M., Alexanderson, H., Astakhov, V., Clarke, G.K.C., Henriksen, M., Hjort, C., Krinner, G., Lunkka, J.P., Möller, P., Murray, A., Nikolskaya, O., Saarnisto, M., Svendsen, J.I., 2004. Ice-dammed lakes and rerouting of the drainage of northern Eurasia during the Last Glaciation. Quat. Sci. Rev. 23, 1313–1332. doi:10.1016/j.quascirev.2003.12.009

Meierbachtol, T., Harper, J., Humphrey, N., 2013. Basal Drainage System Response to Increasing Surface Melt on the Greenland Ice Sheet. Science 341, 777–779.

Newton, A.M.W., Huuse, M., 2017. Glacial geomorphology of the central Barents Sea: Implications for the dynamic deglaciation of the Barents Sea Ice Sheet. Mar. Geol. 387, 114–131. doi:10.1016/j.margeo.2017.04.001

Nitsche, F.O., Gohl, K., Larter, R.D., Hillenbrand, C.D., Kuhn, G., Smith, J.A., Jacobs, S., Anderson, J.B., Jakobsson, M., 2013. Paleo ice flow and subglacial meltwater dynamics in Pine Island Bay, West Antarctica. Cryosphere 7, 249–262. doi:10.5194/tc-7-249-2013

Patton, H., Hubbard, A., Glasser, N.F., Bradwell, T., Golledge, N.R., 2013a. The last Welsh Ice Cap: Part 2 - Dynamics of a topographically controlled icecap. Boreas 42, 491–510. doi:10.1111/j.1502-3885.2012.00301.x

Patton, H., Hubbard, A., Bradwell, T., Glasser, N.F., Hambrey, M.J., Clark, C.D., 2013b. Rapid marine deglaciation: Asynchronous retreat dynamics between the Irish Sea Ice Stream and terrestrial outlet glaciers. Earth Surf. Dyn. 1, 53–65. doi:10.5194/esurf-1-53-2013

Patton, H., Andreassen, K., Bjarnadóttir, L.R., Dowdeswell, J.A., Winsborrow, M.C.M., Noormets, R., Polyak, L., Auriac, A., Hubbard, A., 2015. Geophysical constraints on the dynamics and retreat of the Barents Sea Ice Sheet as a palaeo-benchmark for models of marine ice-sheet deglaciation. Rev. Geophys. 53, 1–31. doi:10.1002/2014RG000468

Patton, H., Hubbard, A., Andreassen, K., Winsborrow, M.C.M., Stroeven, A.P., 2016. The build-up, configuration, and dynamical sensitivity of the Eurasian ice-sheet complex to Late Weichselian climatic and oceanic forcing. Quat. Sci. Rev. 153, 97–121. doi:10.1016/j.quascirev.2016.10.009

Patton, H., Hubbard, A., Andreassen, K., Auriac, A., Whitehouse, P.L., Stroeven, A.P., Shackleton, C., Winsborrow, M.C.M., Heyman, J., Hall, A.M., 2017a. Deglaciation of the Eurasian ice sheet complex. Quat. Sci. Rev. 169, 148–172. doi:10.1016/j.quascirev.2017.05.019

Patton, H., Hubbard, A., Bradwell, T., Schomacker, A., 2017b. The configuration, sensitivity and rapid retreat of the Late Weichselian Icelandic ice sheet. Earth-Science Rev. 166, 223–245. doi:10.1016/j.earscirev.2017.02.001

Pattyn, F., 2008. Investigating the stability of subglacial lakes with a full Stokes ice-sheet model. J. Glaciol. 54, 353–361. doi:10.3189/002214308784886171

Pattyn, F., Perichon, L., Aschwanden, A., Breuer, B., de Smedt, B., Gagliardini, O., Gudmundsson, G.H., Hindmarsh, R.C.A., Hubbard, A., Johnson, J. V., Kleiner, T., Konovalov, Y., Martin, C., Payne, A. J., Pollard, D., Price, S., Rückamp, M., Saito, F., Souček, O., Sugiyama, S., Zwinger, T., 2008. Benchmark experiments for higher-order and full-Stokes ice sheet models (ISMIP–HOM). Cryosph. 2, 95–108. doi:10.5194/tc-2-95-2008

Pedrosa, M.T., Camerlenghi, A., De Mol, B., Urgeles, R., Rebesco, M., Lucchi, R.G., 2011. Seabed morphology and shallow sedimentary structure of the Storfjorden and Kveithola trough-mouth fans (North West Barents Sea). Mar. Geol. 286, 65–81. doi:10.1016/j.margeo.2011.05.009

Piasecka, E.D., Winsborrow, M.C.M., Andreassen, K., Stokes, C.R., 2016. Reconstructing the retreat dynamics of the Bjørnøyrenna Ice Stream based on new 3D seismic data from the central Barents Sea. Quat. Sci. Rev. 151, 212–227. doi:10.1016/j.quascirev.2016.09.003

Piper, D.J.W., Normark, W.R., 2009. Processes That Initiate Turbidity Currents and Their Influence on Turbidites: A Marine Geology Perspective. J. Sediment. Res. 79, 347–362. doi:10.2110/jsr.2009.046

Sergienko, O. V., Hulbe, C.L., 2011. “Sticky spots” and subglacial lakes under ice streams of the Siple Coast, Antarctica. Ann. Glaciol. 52, 18–22. doi:10.3189/172756411797252176

Sharp, M., Richards, K., Willis, I., Arnold, N., Nienow, P., Lawson, W., Tison, J.-L., 1993. Geometry, bed topography and drainage system structure of the haut glacier d’Arolla, Switzerland. Earth Surf. Process. Landforms 18, 557–571. doi:10.1002/esp.3290180608

Shreve, R.L., 1972. The movement of water in glaciers. J. Glaciol. 11, 205–214.

Siegert, M.J., 2000. Antarctic subglacial lakes. Earth Sci. Rev. 50, 29–50. doi:10.1016/S0012-8252(99)00068-9

Siegert, M.J., Le Brocq, A., Payne, A.J., 2007. Hydrological connections between Antarctic subglacial lakes, the flow of water beneath the East Antarctic Ice Sheet and implications for sedimentary processes. Glacial Sediment. Process. Prod. 39, 3–10. doi:10.1002/9781444304435.ch1

Siegfried, M.R., Fricker, H.A., Carter, S.P., Tulaczyk, S., 2016. Episodic ice velocity fluctuations triggered by a subglacial flood in West Antarctica. Geophys. Res. Lett. 43, 2640–2648. doi:10.1002/2016GL067758

Simkins, L.M., Anderson, J.B., Greenwood, S.L., Gonnermann, H.M., Prothro, L.O., Ruth, A., Halberstadt, W., Stearns, L.A., Pollard, D., Deconto, R.M., 2017. Anatomy of a meltwater drainage system beneath the ancestral East Antarctic ice sheet. Nat. geo 10, 691–698. doi:10.1038/NGEO3012

Smith, B.E., Gourmelen, N., Huth, A., Joughin, I., 2017. Connected subglacial lake drainage beneath Thwaites Glacier, West Antarctica. Cryosph. 11, 451–467. doi:10.5194/tc-11-451-2017

Stearns, L. A., Smith, B.E., Hamilton, G.S., 2008. Increased flow speed on a large East Antarctic outlet glacier caused by subglacial floods. Nat. Geosci. 1, 827–831. doi:10.1038/ngeo356

Stroeven, A.P., Hättestrand, C., Kleman, J., Heyman, J., Fabel, D., Fredin, O., Goodfellow, B.W., Harbor, J.M., Jansen, J.D., Olsen, L., Caffee, M.W., Fink, D., Lundqvist, J., Rosqvist, G.C., Strömberg, B., Jansson, K.N., 2016. Deglaciation of Fennoscandia. Quat. Sci. Rev. 147, 91–121. doi:10.1016/j.quascirev.2015.09.016

Thomsen, H., Olesen, O., Braithwaite, R.J., Boggild, C., 1991. Ice drilling and mass balance at Pakitsoq, Jakobshavn, central West Greenland. Rep. Geol. Surv. Greenl. 152, 80–84.

Trommelen, M.S., Ross, M., Ismail, A., 2014. Ribbed moraines in northern Manitoba, Canada: Characteristics and preservation as part of a subglacial bed mosaic near the core regions of ice sheets. Quat. Sci. Rev. 87. doi:10.1016/j.quascirev.2014.01.010

Tulaczyk, S., Kamb, W.B., Engelhardt, H.F., 2000. Basal mechanics of Ice Stream B, west Antarctica: 1. Till mechanics. J. Geophys. Res. 105, 463–481. doi:10.1029/1999JB900329

Vaughan, D.G., Corr, H.F.J., Smith, A.M., Pritchard, H.D., Shepherd, A., 2008. Flow-switching and water piracy between Rutford Ice Stream and Carlson Inlet , West Antarctica. J. Glaciol. 54, 41–48.

Vorren, T.O., Landvik, J., Andreassen, K., Laberg, J.S., 2011. Glacial History of the Barents Sea Region, 1st ed, Quaternary Glaciations - Extent and Chronology. Elsevier Inc. doi:10.1016/B978-0-444-53447-7.00027-1

Waelbroeck, C., Labeyrie, L., Michel, E., Duplessy, J.C., McManus, J.F., Lambeck, K., Balbon, E., Labracherie, M., 2002. Sea-level and deep water temperature changes derived from benthic foraminifera isotopic records. Quat. Sci. Rev. 21, 295–305. doi:10.1016/S0277-3791(01)00101-9

Weertman, J., 1972. General theory of water flow at the base of a glacier or ice sheet. Rev. Geophys. 10, 287–333.

Winberry, J.P., Anandakrishnan, S., Alley, R.B., 2009. Seismic observations of transient subglacial water-flow beneath MacAyeal Ice Stream, West Antarctica. Geophys. Res. Lett. 36, 1–5. doi:10.1029/2009GL037730

Wingham, D.J., Siegert, M.J., Shepherd, A., Muir, A.S., 2006. Rapid discharge connects Antarctic subglacial lakes. Nature 440, 1033–1036. doi:10.1038/nature04660

Winsborrow, M., Andreassen, K., Hubbard, A., Plaza-Faverola, A., Gudlaugsson, E., Patton, H., 2016. Regulation of ice stream flow through subglacial formation of gas hydrates. Nat. Geosci. 9, 370-374. doi:10.1038/ngeo2696

Wright, A., Siegert, M., 2012. A fourth inventory of Antarctic subglacial lakes. Antarct. Sci. 24, 1–6. doi:10.1017/S095410201200048X

Wright, A.P., Siegert, M.J., Le Brocq, A.M., Gore, D.B., 2008. High sensitivity of subglacial hydrological pathways in Antarctica to small ice-sheet changes. Geophys. Res. Lett. 35, L17504. doi:10.1029/2008GL034937

Wright, P.J., Harper, J.T., Humphrey, N.F., Meierbachtol, T.W., 2016. Measured basal water pressure variability of the western Greenland Ice Sheet: Implications for hydraulic potential. J. Geophys. Res. Earth Surf. 121, 1134–1147. doi:10.1002/2016JF003819.Received

Xu, Y., Rignot, E., Menemenlis, D., Koppes, M., 2012. Numerical experiments on subaqueous melting of greenland tidewater glaciers in response to ocean warming and enhanced subglacial discharge. Ann. Glaciol. 53, 229–234. doi:10.3189/2012AoG60A139

Figure 1: The Fennoscandian and Barents Sea sectors of the Eurasian Ice Sheet complex. Last Glacial Maximum (LGM) ice extent is drawn in white (Patton et al. 2017a), major troughs are named and the flow directions of their associated palaeo-ice streams are indicated with arrows. Present-day lakes are drawn in blue. Lt. = Lithuania; Lv. = Latvia; Ee. = Estonia; HT = Hinlopen Trough; KvT = Kvitøya trough; FVT = Franz Victoria Trough; SF = Storfjordrenna; DR = Djuprenna; VF/TD = Vestfjorden/Traenadjupet.

Figure 2 (below): Subglacial hydrological evolution of the FIS and BSIS, as snapshots of hydrology in the build up to the LGM **(a-c)**, during the LGM **(d-f)** and during ice retreat **(g-i)**. The Strahler stream order method of calculating downstream connectivity was applied to the predicted water routes and stream width is proportional to this. Subglacial topography is coloured in greyscale, and ice-sheet surface slope is indicated by contours at 400m intervals. The coastline evolves in response to changes in isostatic loading and fluctuations in eustatic sea level; the present-day coastline is shown to aid spatial reference. Subglacial lakes and drainage routing in the Norwegian Channel at 22.7 ka BP were calculated in conjunction with simulated ice covering the British Isles. SGL = Subglacial lake; Lt. = Lithuania; Lv. = Latvia; Ee. = Estonia.

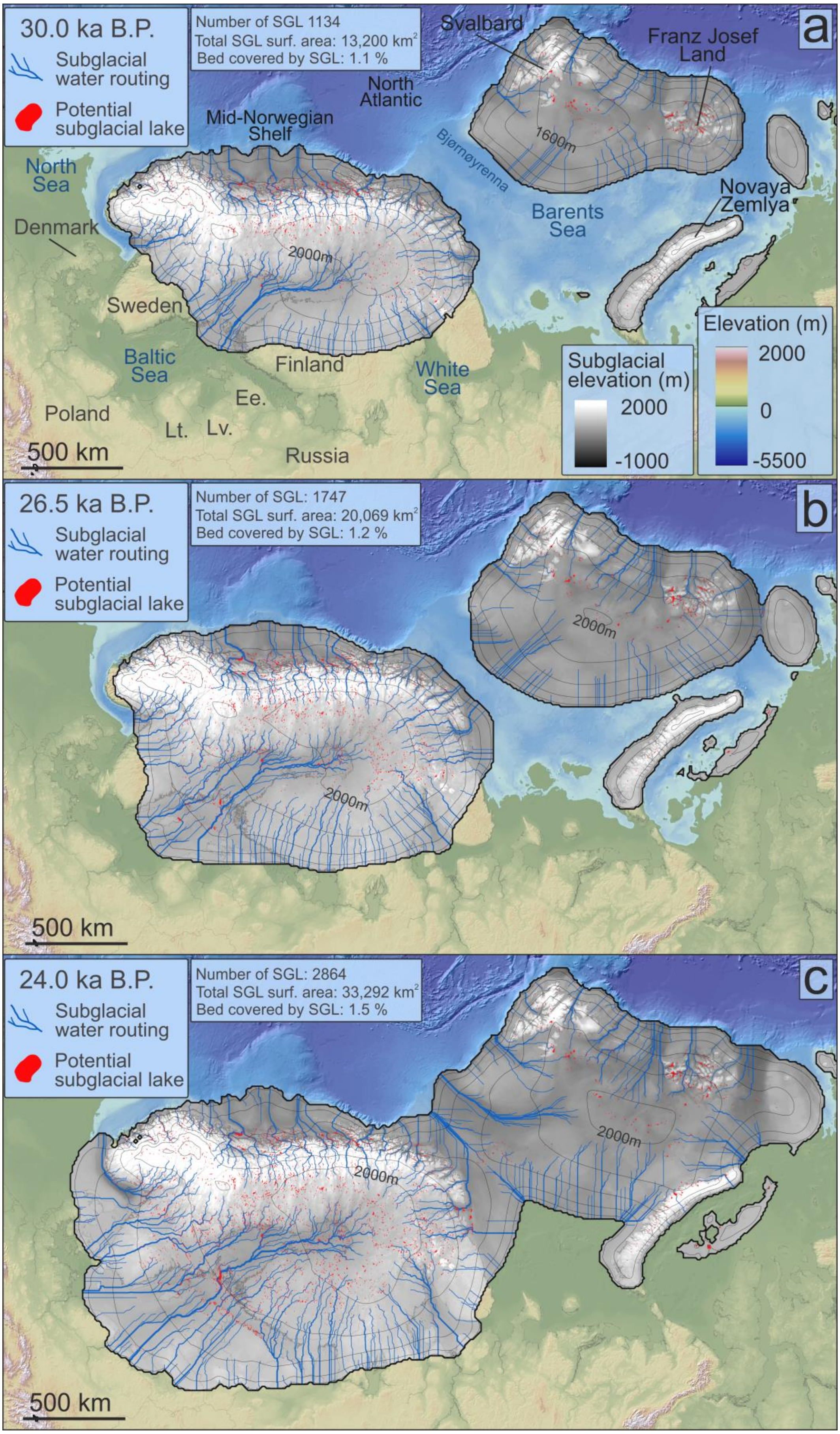
30.0 ka B.P.
Subglacial water routing
Potential subglacial lake
Number of SGL 1134
Total SGL surf. area: 13,200 km²
Bed covered by SGL: 1.1 %
a
Svalbard
Franz Josef Land
North Atlantic
Mid-Norwegian Shelf
Bjørnøyrenna
1600m
North Sea
Denmark
2000m
Barents Sea
Novaya Zemlya
Sweden
Baltic Sea
Finland
White Sea
Ee.
Poland
Lt.
Lv.
Russia
500 km
Subglacial elevation (m)
2000
-1000
Elevation (m)
2000
0
-5500
26.5 ka B.P.
Subglacial water routing
Potential subglacial lake
Number of SGL: 1747
Total SGL surf. area: 20,069 km²
Bed covered by SGL: 1.2 %
b
2000m
2000m
500 km
24.0 ka B.P.
Subglacial water routing
Potential subglacial lake
Number of SGL: 2864
Total SGL surf. area: 33,292 km²
Bed covered by SGL: 1.5 %
c
2000m
2000m
500 km

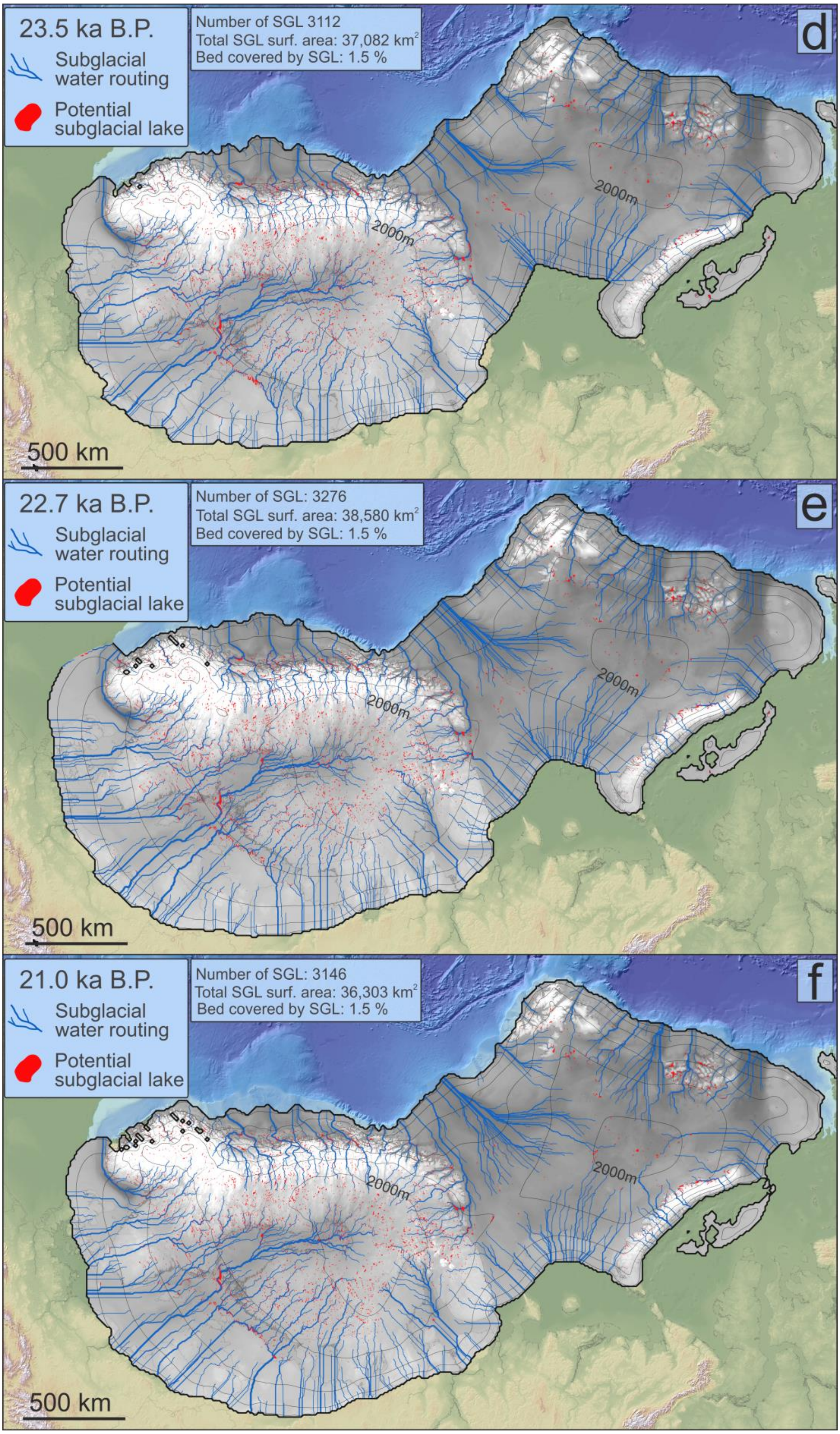

23.5 ka B.P.
Subglacial water routing
Potential subglacial lake
Number of SGL 3112
Total SGL surf. area: 37,082 km^2
Bed covered by SGL: 1.5 %
d
2000m
2000m
500 km
22.7 ka B.P.
Subglacial water routing
Potential subglacial lake
Number of SGL: 3276
Total SGL surf. area: 38,580 km^2
Bed covered by SGL: 1.5 %
e
2000m
2000m
500 km
21.0 ka B.P.
Subglacial water routing
Potential subglacial lake
Number of SGL: 3146
Total SGL surf. area: 36,303 km^2
Bed covered by SGL: 1.5 %
f
2000m
2000m
500 km

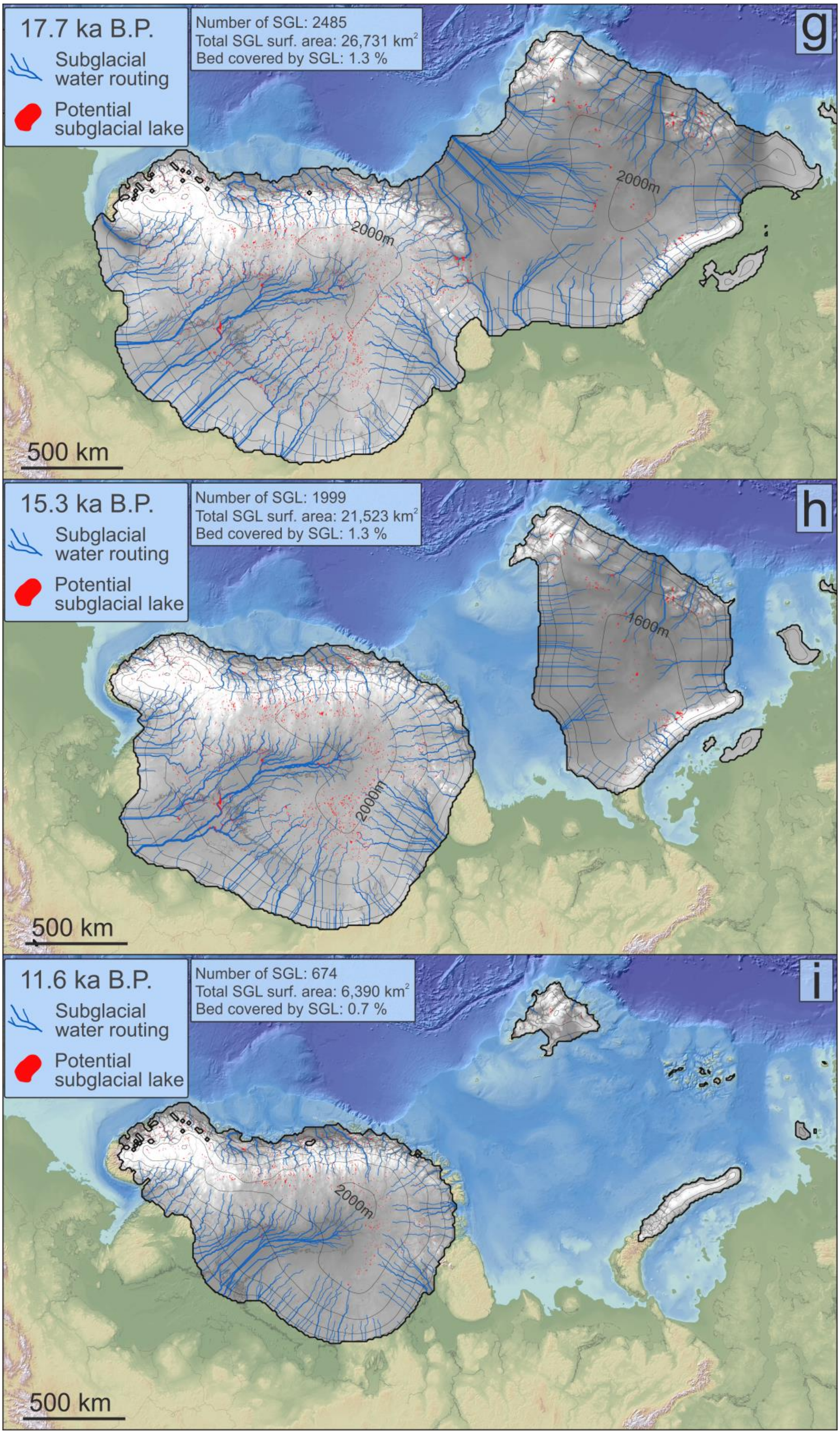
17.7 ka B.P.
Subglacial water routing
Potential subglacial lake
Number of SGL: 2485
Total SGL surf. area: 26,731 km²
Bed covered by SGL: 1.3 %
g
2000m
2000m
500 km
15.3 ka B.P.
Subglacial water routing
Potential subglacial lake
Number of SGL: 1999
Total SGL surf. area: 21,523 km²
Bed covered by SGL: 1.3 %
h
1600m
2000m
500 km
11.6 ka B.P.
Subglacial water routing
Potential subglacial lake
Number of SGL: 674
Total SGL surf. area: 6,390 km²
Bed covered by SGL: 0.7 %
i
2000m
500 km

Figure 3 (below): Subglacial lake persistency shows the percentage of time that subglacial lakes formed while ice covered in **(a)** the Barents Sea and **(b)** Fennoscandia. The surface area of the different persistency classes is also plotted. The omitted category of 1-10% persistency covers surface areas of 22,166 km^2 over Fennoscandia, and 17,869 km^2 for the Barents Sea region. BIS = Baltic Ice Stream; Dr = Djuprenna; FVT = Franz Victoria Trough; KvT = Kvitøya trough; SF = Storfjordrenna; Vf/Td = Vestfjorden/Traenadjupet.

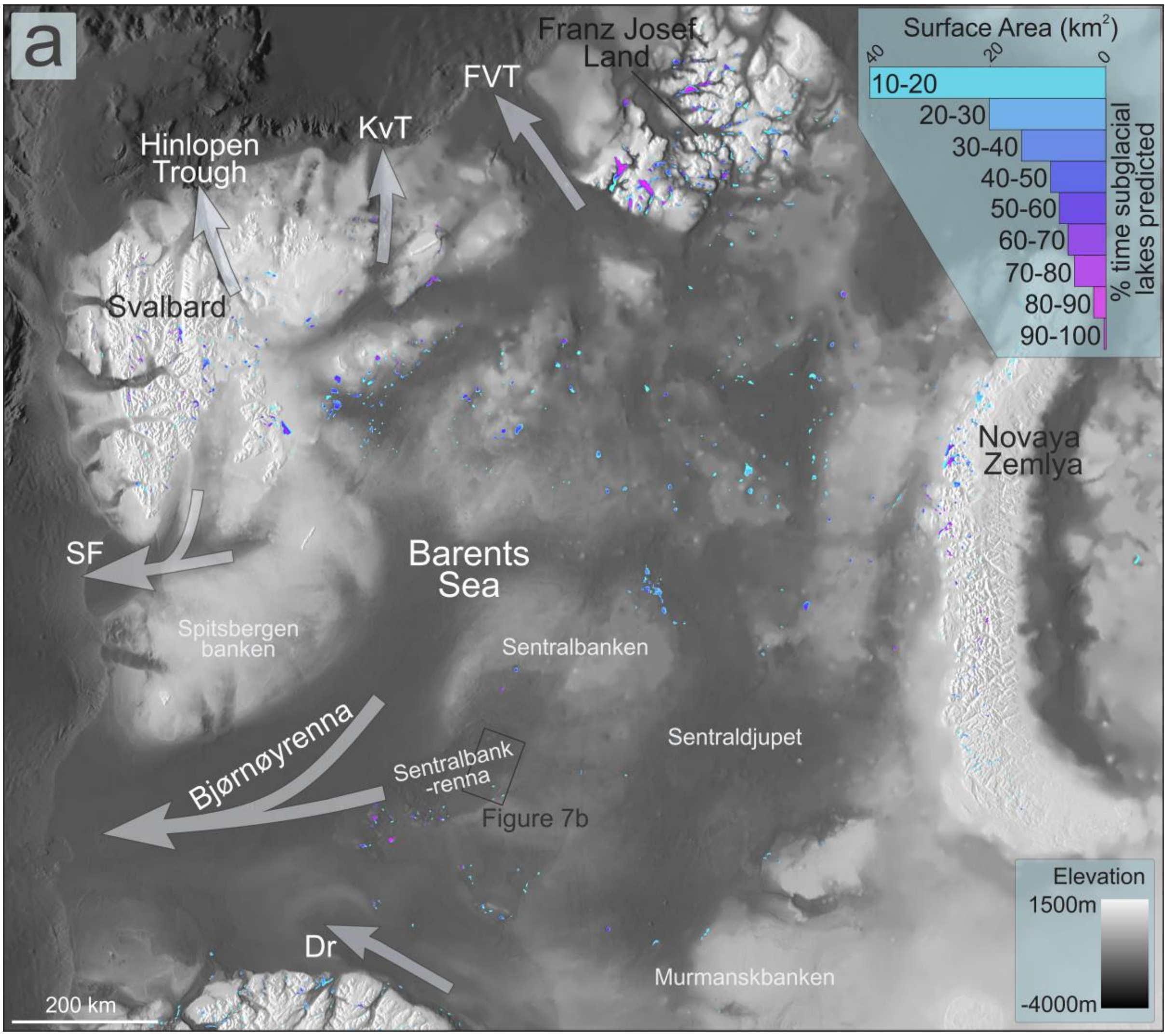

Figure 3 (below): continued…

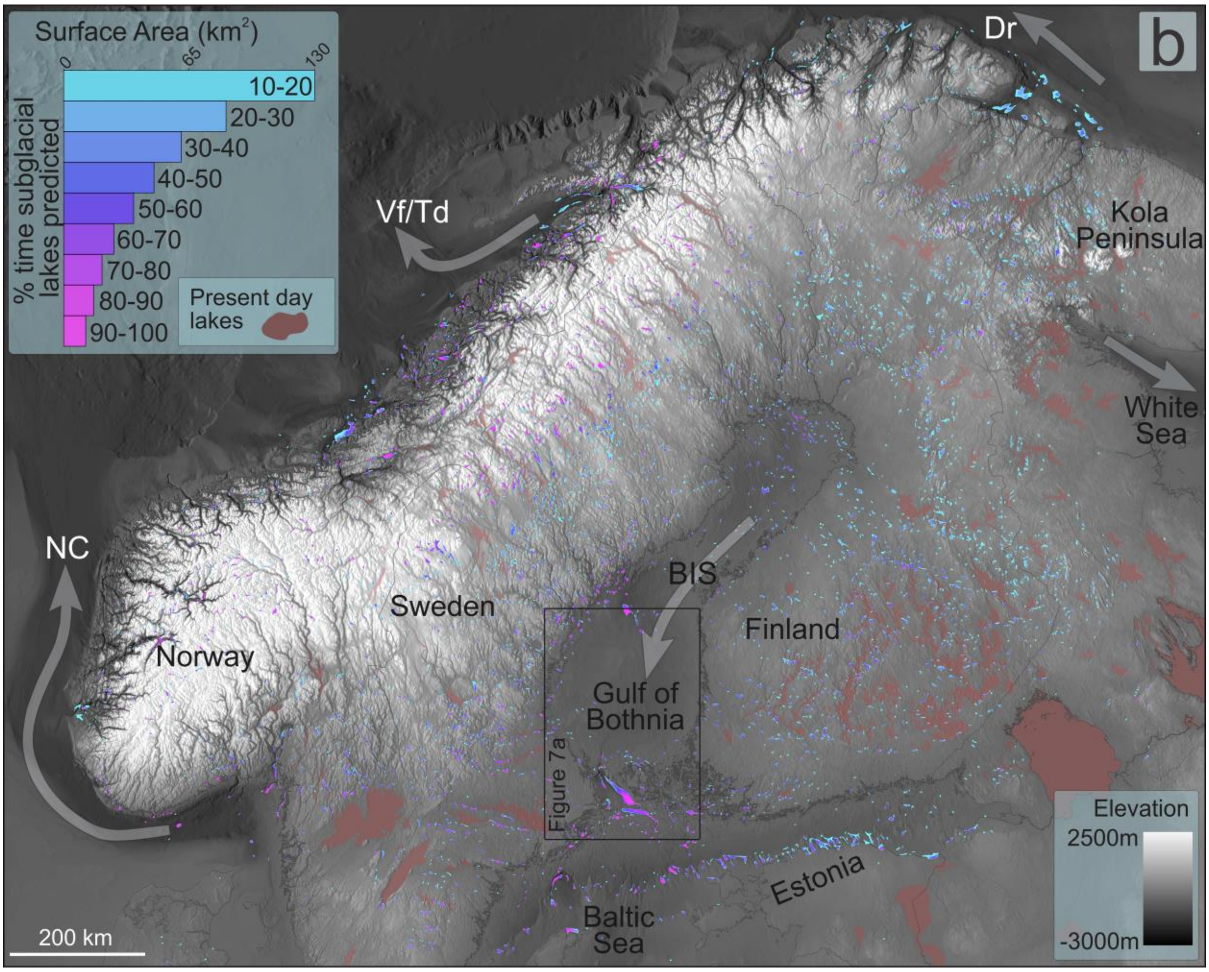

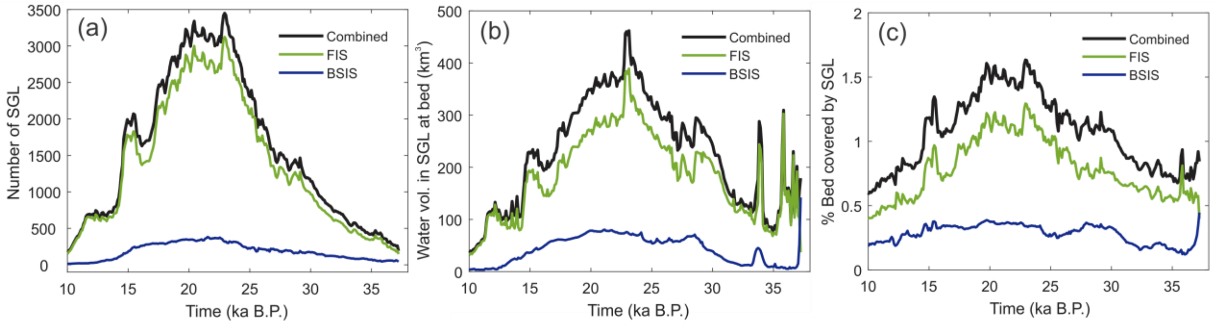

Figure 4: **(a)** Total number of potential subglacial lakes, **(b)** estimated volumes of water stored within subglacial lakes, and **(c)** the predicted percentage of the bed occupied by subglacial lakes, for the BSIS, FIS, and combined from 37-10 ka BP.

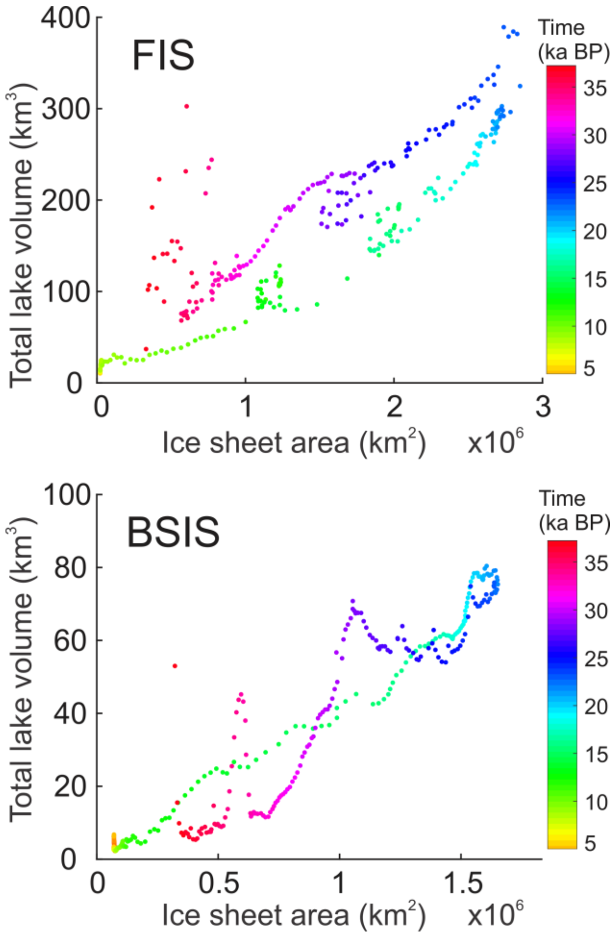

Figure 5: Estimated total volume of water stored within subglacial lakes beneath the FIS and BSIS plotted against ice sheet areal extent. Points are coloured chronologically. A small number of timeslices with total water storage volumes greater than 100 km^3 for the BSIS are omitted in order to better present the overall trends in the data.

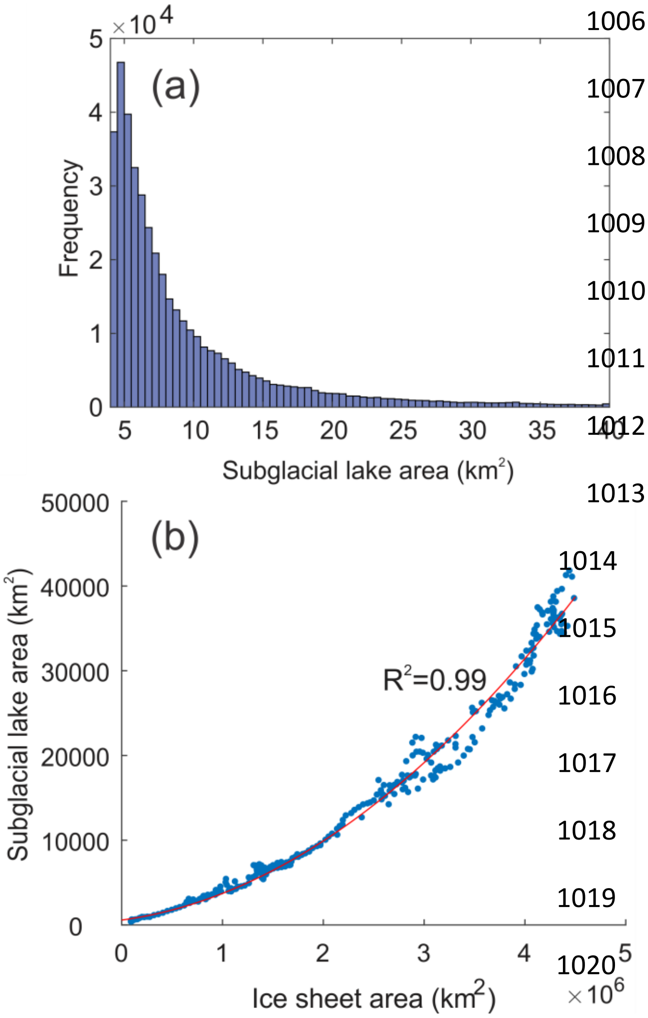

Figure 6: (a) Subglacial lake size-frequency histogram for all lakes predicted through the Late Weichselian glaciation. **(b)** Total subglacial lake area plotted against ice sheet area.

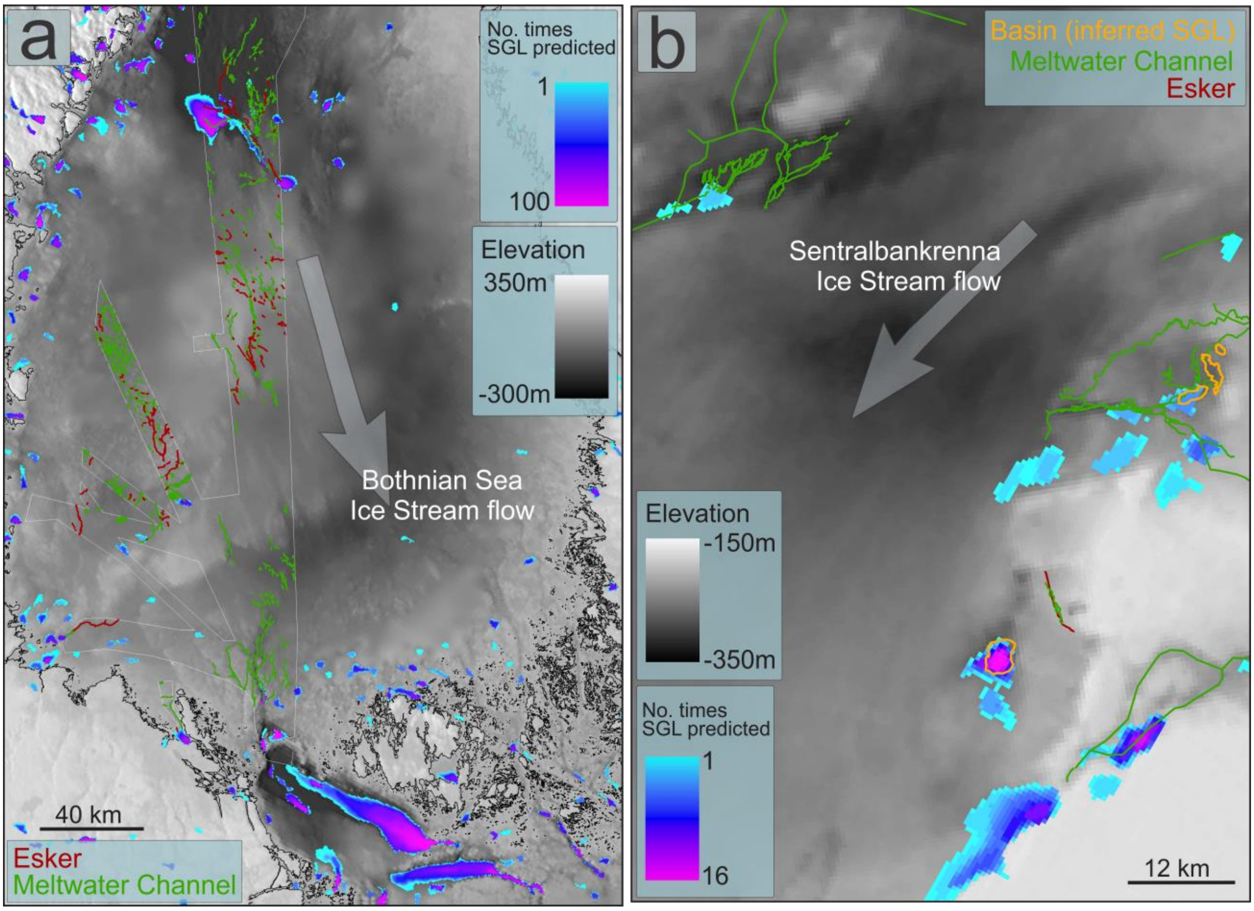

Figure 7: Potential subglacial lakes predicted in this study compared to published mapping of subglacial meltwater geomorphology in **(a)** the Gulf of Bothnia (Greenwood et al., 2017, 2016) and **(b)** the central Barents Sea (Bjarnadóttir et al., 2017; Esteves et al., *In Review*, 2017). The outline of the bathymetric dataset upon which the mapping in the Gulf of Bothnia is based is drawn in white. Ice stream flow direction arrows are drawn based on the published reconstructions of ice flow.

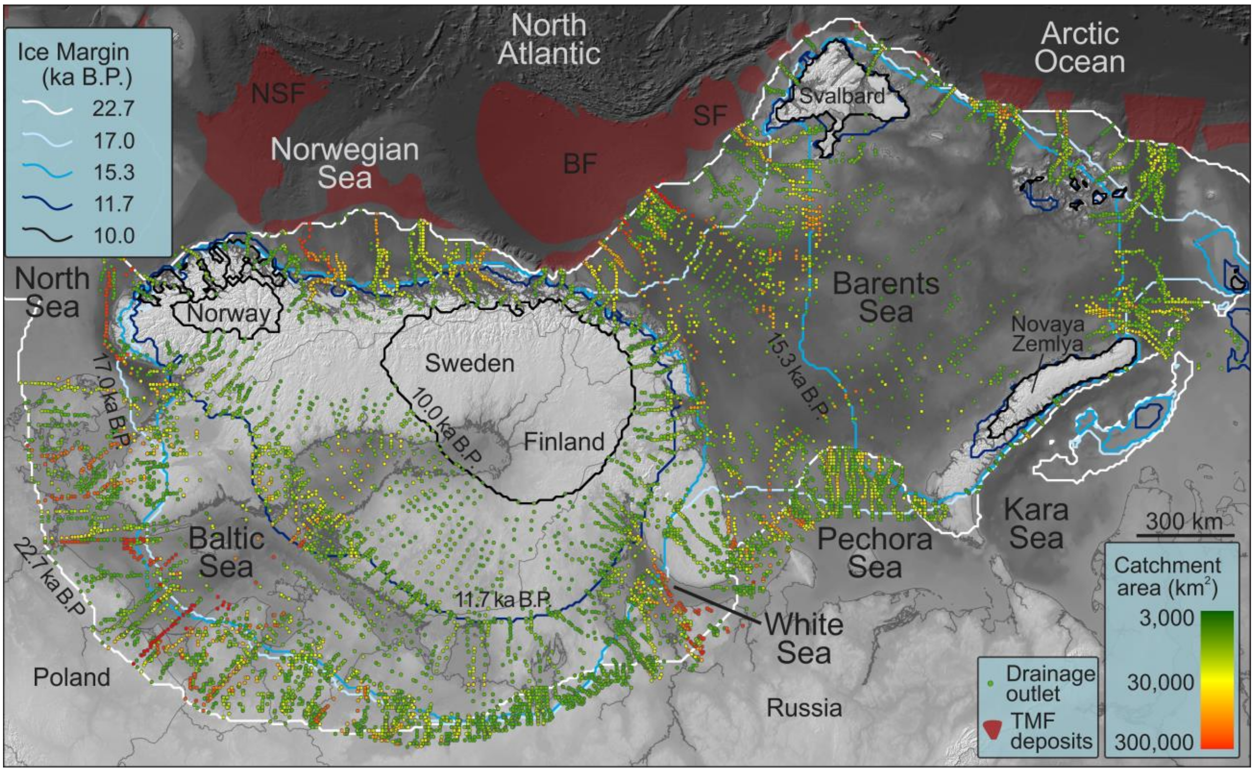

Figure 8: Subglacial catchment outlet migration between maximum ice extent conditions (22.7 ka BP) and 10 ka BP at 100-year intervals. The outlets are coloured according to the size of their associated catchment on a logarithmic scale. Outlets for small catchments (< 3000 km^2) have been removed. The extents of major trough mouth fan deposits are shown in red. BF = Bjørnøyrenna Fan; NSF = North Sea Fan; SF = Storfjordrenna Fan. Ice margin extents are derived from the ice sheet model (Patton et al., 2017a).

Sensitivity parameter	Total subglacial lake area (km^2)	Area intersecting with optimum (%)
F = 0.7	177,902	88
F = 0.8	108,269	92
F = 0.925	36,303	100
F = 1	9018	42
Bf x 0	57,793	97
Bf x 1	36,303	100
Bf x 2	32,935	92
Bf x 3	30,315	86
Bt = no mask	36,303	100
Bt <= -1.5°C	20,202	58
Bt <= -0.75°C	17,601	51
Bt <= 0°C	10,891	31
A_0 = 5	48,144	76
A_0 = 25	39,279	91
A_0 = 50	36,303	100
A_0 = 75	36,026	94

Table 1: Total potential subglacial lake area occupying the bed under an LGM (21 ka BP) timeslice following perturbations in the flotation factor (F), bed filtering (Bf), bed temperature masks below the pressure melting point (Bt) and ice flow enhancement factor perturbations (A0) relative to the pressure melting point.

8.0 Supplementary material

Table S1: The GEBCO data source used for gridding the DEM underlying predicted subglacial lakes beneath the 21 ka BP timeslice. The total number of subglacial lakes predicted from this timeslice is 3146, of which 2800 are beneath the FIS and 346 beneath the BIS.

GEBCO source (file code)	FIS subglacial lakes	%	BIS subglacial lakes	%
Constrained by bathymetric sounding (-9999)	0	0	1	0
Terrestrial grid point (-8888)	2091	75	104	30
Interpolated (0)	20	1	0	0
Interpolated point from IBCAO V3 grid (1900)	60	2	54	16
Multibeam data (1910)	57	2	5	1
Single beam data from IBCAO V3 (1920)	29	1	58	17
Depth contours from digitised charts (1950)	1	0	71	21
Olex data (2000)	88	3	53	15
Interpolated (2100)	2	0	0	0
EMODnet 2013 Grid (3800)	43	2	0	0
Baltic Sea Bathymetry Database grid (3900)	409	15	0	0

Figure S1 (a-i) (below): Potential subglacial lakes and drainage routes at 21 ka BP following perturbations in the flotation factor (F), bed filtering (Bf), bed temperature masks below the pressure melting point (Bt), and flow enhancement factor (A_0).

Figure S1: Potential subglacial lakes and drainage routes at 21 ka BP following perturbations in the flotation factor (F), bed filtering (Bf), bed temperature masks below the pressure melting point (Bt), and the flow enhancement factor (A_0).

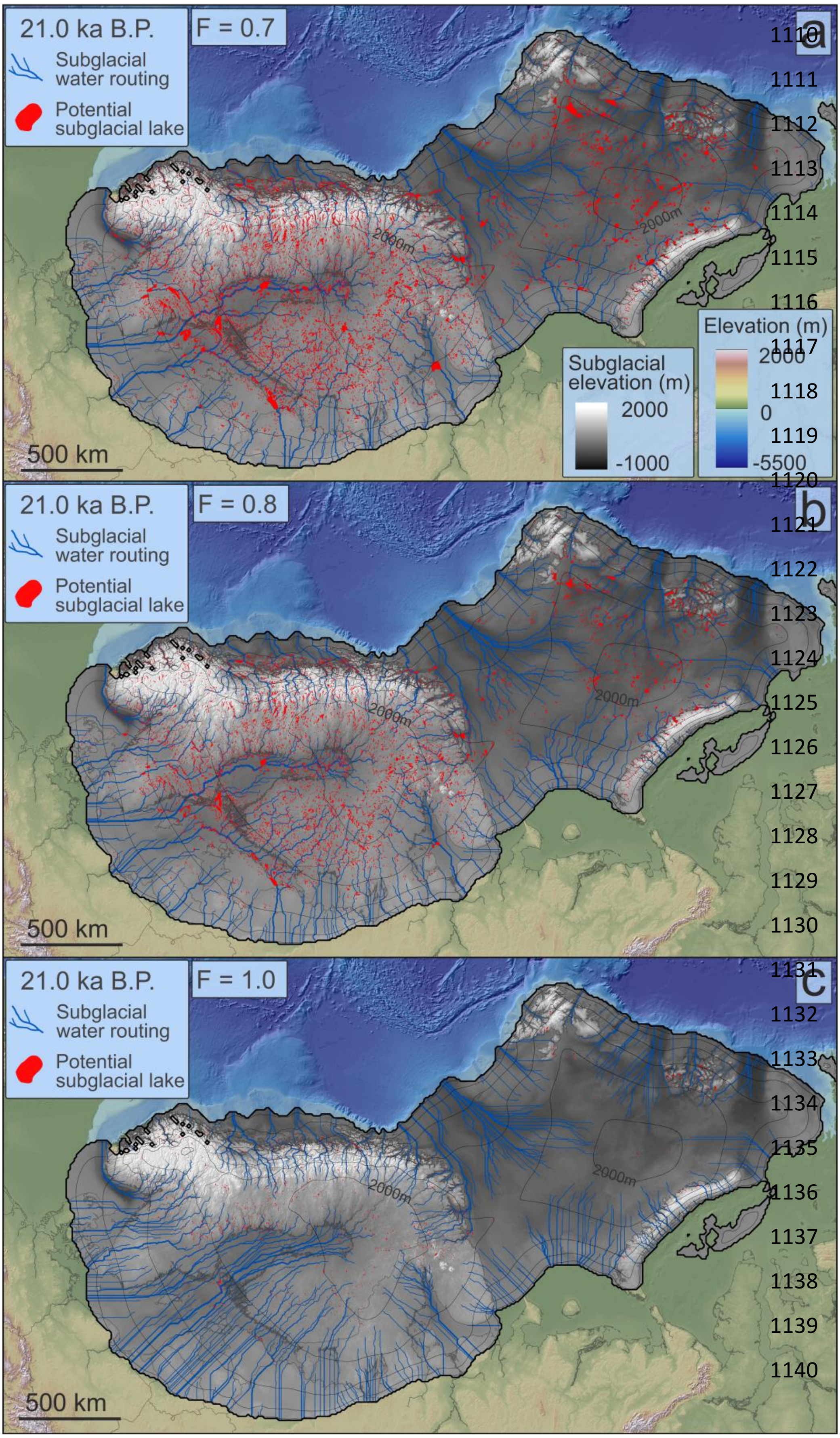

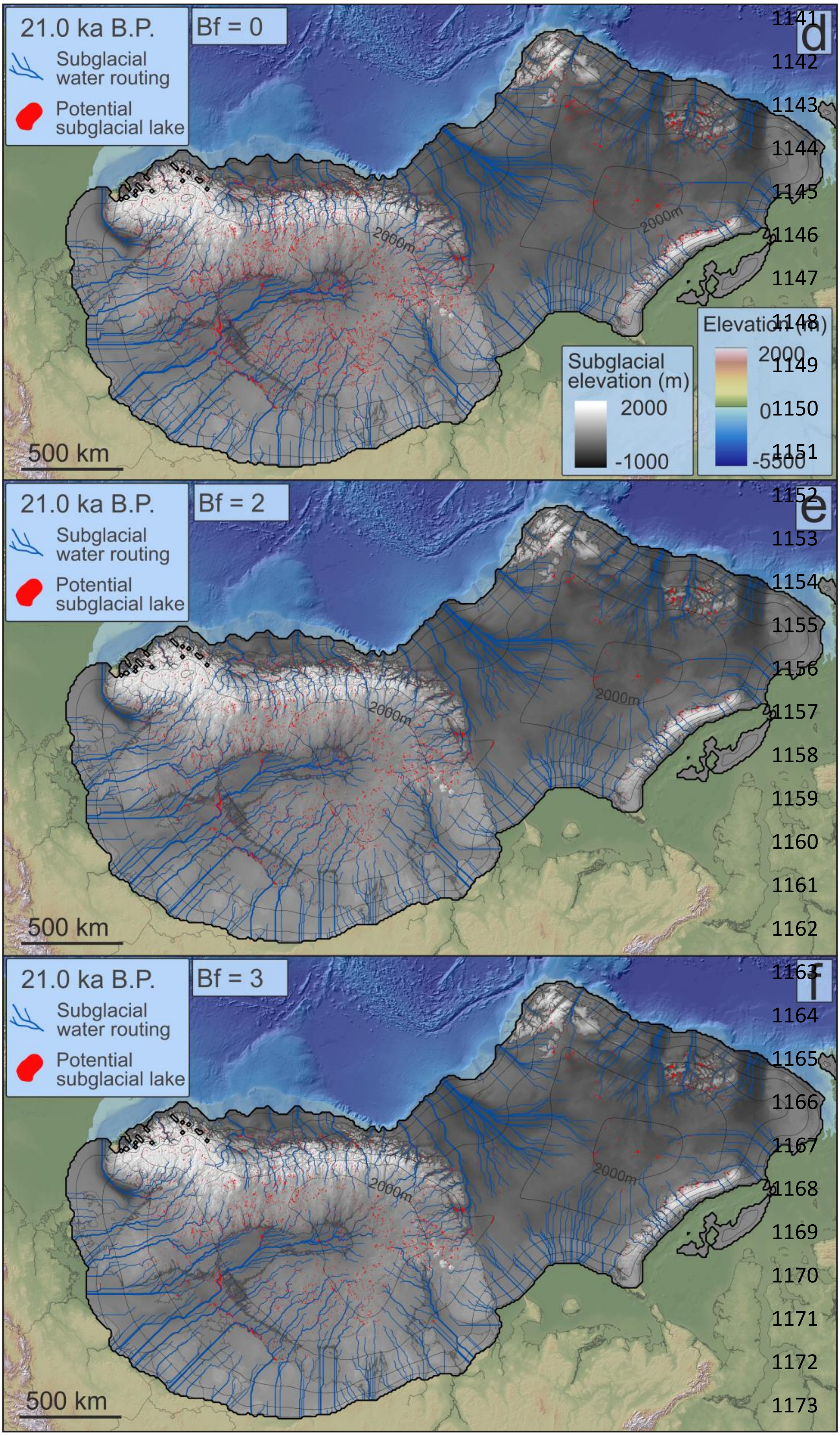

21.0 ka B.P.
Bf = 0
Subglacial water routing
Potential subglacial lake
d
2000m
2000m
Subglacial elevation (m)
2000
-1000
Elevation (m)
2000
0
-5500
500 km
21.0 ka B.P.
Bf = 2
Subglacial water routing
Potential subglacial lake
e
2000m
2000m
500 km
21.0 ka B.P.
Bf = 3
Subglacial water routing
Potential subglacial lake
f
2000m
2000m
500 km

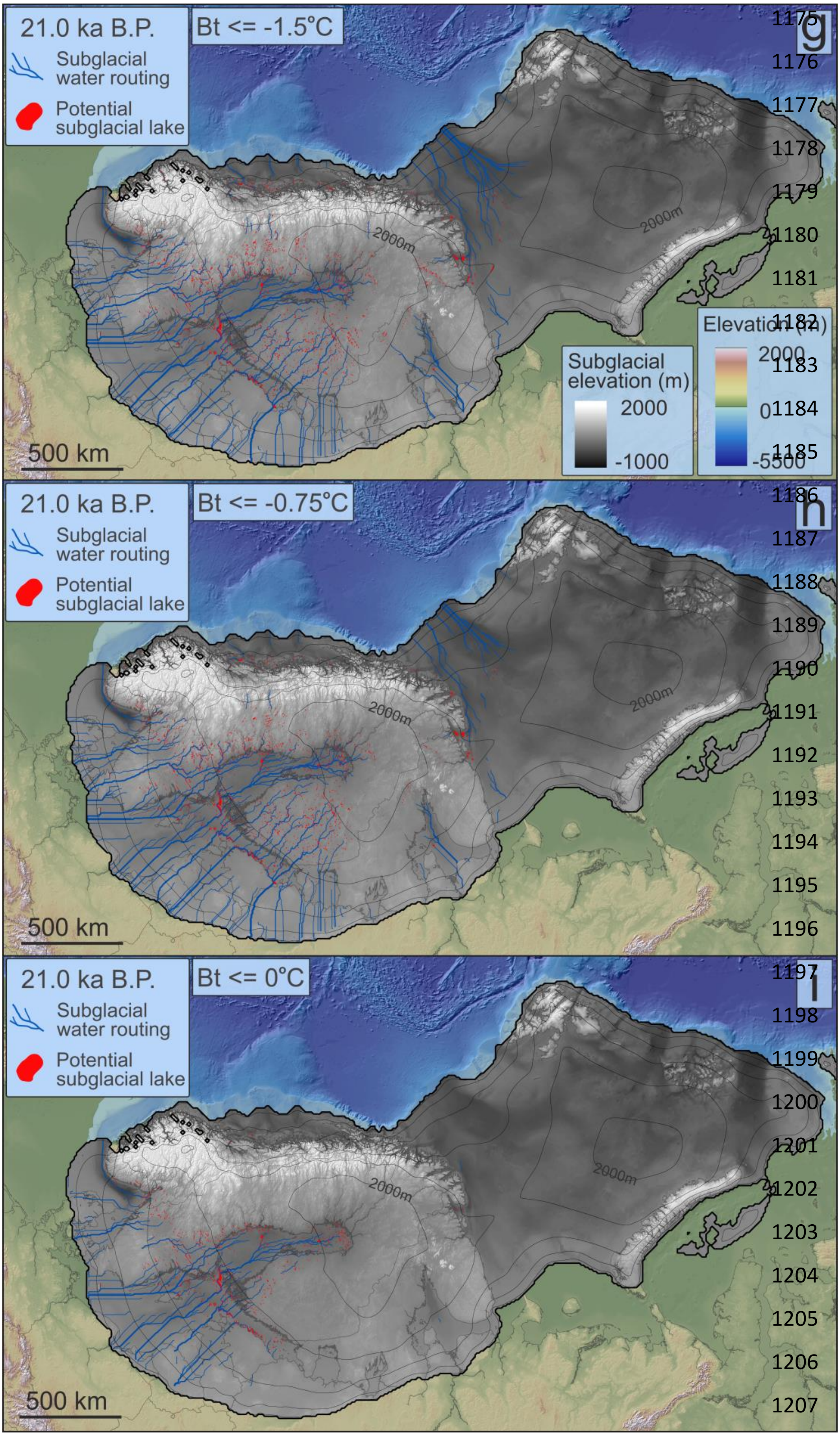
21.0 ka B.P.
Bt <= -1.5°C
g
Subglacial water routing
Potential subglacial lake
2000m
2000m
Subglacial elevation (m)
2000
-1000
Elevation (m)
2000
0
-5500
500 km
21.0 ka B.P.
Bt <= -0.75°C
h
Subglacial water routing
Potential subglacial lake
2000m
2000m
500 km
21.0 ka B.P.
Bt <= 0°C
i
Subglacial water routing
Potential subglacial lake
2000m
2000m
500 km

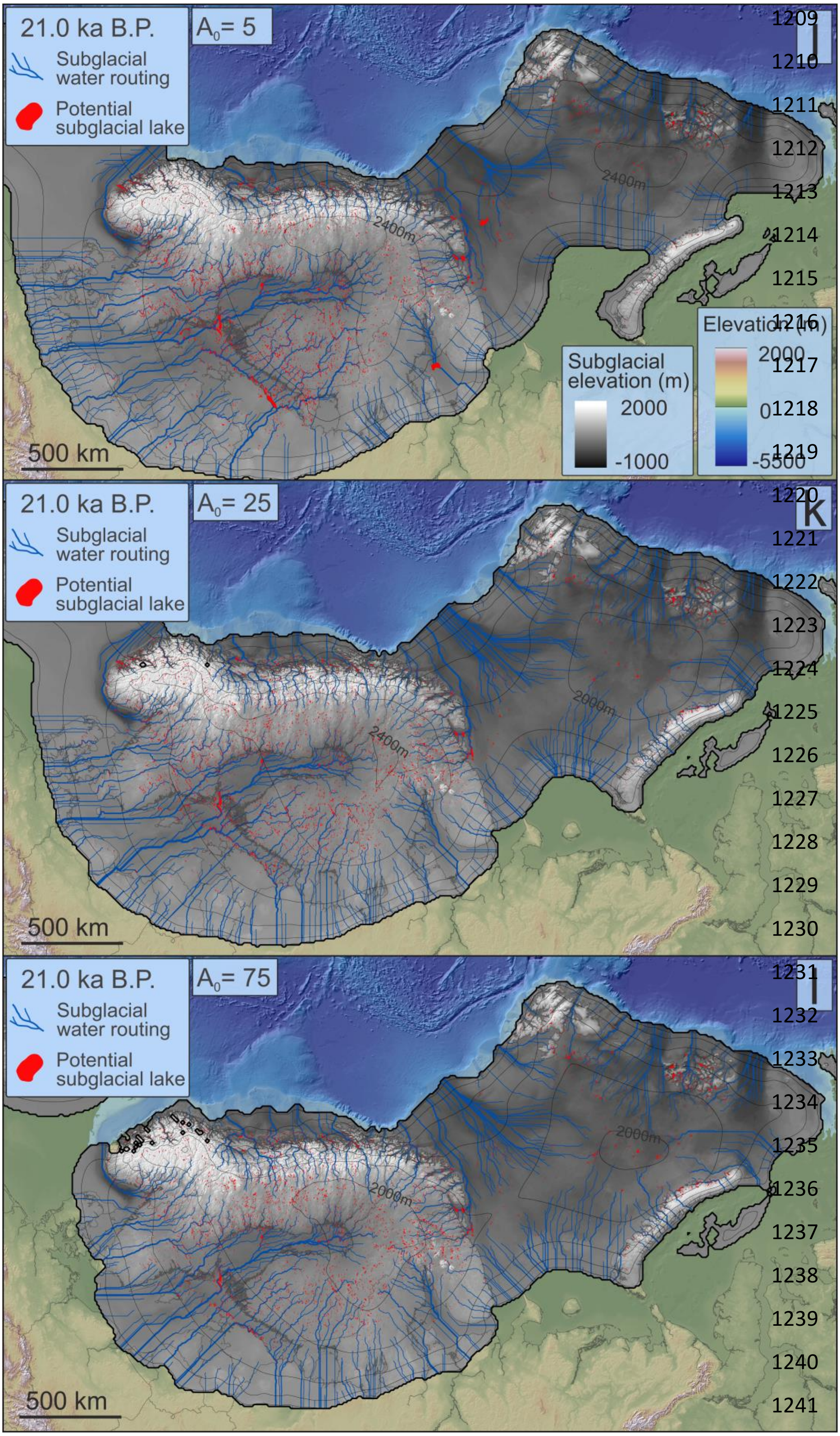
21.0 ka B.P.
A_0= 5
Subglacial water routing
Potential subglacial lake
2400m
Subglacial elevation (m)
2000
-1000
Elevation (m)
2000
0
-5500
500 km
21.0 ka B.P.
A_0= 25
Subglacial water routing
Potential subglacial lake
2400m
2000m
K
500 km
21.0 ka B.P.
A_0= 75
Subglacial water routing
Potential subglacial lake
2000m
500 km